Vapor flows condensing at incidence onto a plane condensed phase in the presence of a noncondensable gas. I. Subsonic condensation

Satoshi Taguchi and Kazuo Aoki[a)]
Department of Aeronautics and Astronautics, Graduate School of Engineering, Kyoto University, Kyoto 606-8501, Japan

Shigeru Takata[b)]
Département de Mathématiques et Applications, École Normale Supérieure, 45, rue d'Ulm, 75230 Paris Cedex 05, France

(Received 22 July 2002; accepted 2 December 2002; published 30 January 2003)

A steady flow of a vapor in a half space condensing onto a plane condensed phase of the vapor at incidence is considered in the case where another gas that neither evaporates nor condenses (the noncondensable gas) is present near the condensed phase. The behavior of the vapor and noncondensable gas is investigated on the basis of kinetic theory under the assumption that the molecules of the noncondensable gas are mechanically identical with those of the vapor. In particular, the relation, among the parameters of the vapor at infinity (the pressure, temperature, and flow velocity of the vapor), those related to the condensed phase (the temperature of the condensed phase and the corresponding saturation pressure of the vapor), and the amount of the noncondensable gas, that admits a steady solution is obtained numerically by the use of a model Boltzmann equation proposed by Garzó *et al.* [Phys. Fluids A **1**, 380 (1989)]. The present analysis is the continuation of an earlier work by Sone *et al.* [Transp. Theory Stat. Phys. **21**, 297 (1992)], where the case in which the vapor flow is condensing perpendicularly onto the condensed phase is investigated exclusively. The case with subsonic condensation is discussed in the present paper (the case with supersonic condensation is left to the subsequent paper). © *2003 American Institute of Physics.* [DOI: 10.1063/1.1539476]

I. INTRODUCTION

The half-space problem of strong evaporation and condensation, more specifically, steady flows of a vapor condensing onto or evaporating from a plane condensed phase of the vapor with a high evaporation or condensation rate, has been one of the important subjects in kinetic theory of gases in the following aspects.

(i) In spite of the fact that it appears to be the simplest boundary-value problem of the full Boltzmann equation, the behavior of the solution is not obvious at all. For example, there is a steady solution only when the parameters of the vapor at infinity (the pressure, temperature, and flow velocity of the vapor) and those associated with the condensed phase (the temperature of the condensed phase and the corresponding saturation pressure of the vapor) satisfy certain relations. Furthermore, the relations are qualitatively different depending on whether the vapor is evaporating or condensing, and furthermore, whether it is condensing with a supersonic speed or a subsonic speed. (See Refs. 1 and 2.)

(ii) The half-space problem also plays an important role in the continuum limit (i.e., the limit where the mean free path of the vapor molecules or the Knudsen number of the system goes to zero) for vapor flows around arbitrarily shaped boundaries, consisting of the condensed phase of the vapor, on which strong evaporation or condensation is taking place. To be more specific, the half-space problem corresponds to the Knudsen-layer problem in this case, and the relations among the parameters mentioned above provide the boundary conditions for the fluid-dynamic equations (the Euler set of equations for a perfect gas). (See Refs. 2 and 3.)

The fact mentioned in (i) was clarified and the parameter relations, together with the behavior of the physical quantities, were obtained by means of intensive numerical analysis (Refs. 4 and 5 for evaporation and Refs. 6, 7, and 5 for condensation) based on the Bhatnagar–Gross–Krook (BGK) model[8–10] of the Boltzmann equation. Some analytical results based on the Boltzmann equation as well as the BGK model are also available for slow evaporation and condensation[1,11] and for transonic condensation.[1,12] We refer to Ref. 13 as a pioneering work and note that numerical methods other than using the BGK model have also been employed to obtain the aforementioned relations (e.g., Refs. 14–17). In addition, it should be mentioned that the entropy inequality (or the H-theorem) was used recently to estimate the relations rigorously.[18,19] The reader is referred to Refs. 1, 2, and 18 for the review on this problem. These numerical and analytical results have induced mathematicians' interest in the rigorous mathematical treatment of the problem. In fact, several successful results on the half-space problem corresponding to the case of evaporation and condensation have been reported so far (e.g., Refs. 20–23).

[a)]Electronic mail: aoki@aero.mbox.media.kyoto-u.ac.jp
[b)]Permanent address: Department of Aeronautics and Astronautics, Graduate School of Engineering, Kyoto University, Kyoto 606-8501, Japan.

The numerical analysis of the half-space problem of strong condensation was extended to the case where another component that does not participate in evaporation or condensation (say, noncondensable gas) is present near the condensed phase.[24,25] The effect of the noncondensable gas on the vapor flows, especially on the relation among the parameters allowing a steady solution, is clarified in these references.

The half-space problem of strong condensation in the presence of a noncondensable gas was revisited recently in connection with the continuum limit of the vapor flows around the boundary, consisting of the condensed phase of the vapor, in the case where a small amount of the noncondensable gas is contained in the system. In Ref. 26, a simple one-dimensional problem, i.e., a vapor flow caused by evaporation and condensation between two parallel plane condensed phases was investigated, and it was pointed out that the noncondensable gas with an infinitesimal average concentration has a significant effect on the vapor flow in the continuum limit. The physical reasoning of this seemingly paradoxical effect is as follows. The infinitesimal amount of the noncondensable gas is concentrated in the thickless Knudsen layer on the condensing surface by the vapor flow, so that its local number density on the surface becomes high enough (comparable to that of the vapor) to affect the vapor flow. The method of analysis employed in Ref. 26 is the systematic asymptotic analysis of the Boltzmann equation for small Knudsen numbers developed by Sone (e.g., Refs. 27–31, and 3; see Refs. 2 and 32 for the summary of the asymptotic theory). Recently, the analysis of Ref. 26 was extended to the case of general geometry.[33] The continuum limit in this situation is outlined as follows. The vapor flow is free from the noncondensable gas except in the Knudsen layer on the boundary where condensation is taking place. Therefore, the fluid-dynamic equations and their boundary condition on the boundary where evaporation is taking place are the same as those in the case without the noncondensable gas,[3] more specifically, the equations are the Euler set of equations for a perfect gas. The thickless Knudsen layer on the condensing boundary may contain the noncondensable gas, as mentioned above. Such Knudsen layer is described by the half-space problem under consideration, i.e., that of strong condensation in the presence of the noncondensable gas. Then, the relation among the parameters allowing the steady solution in the half-space problem, together with the continuity equation of the flow of the noncondensable gas along the boundary (inside the thickless Knudsen layer), gives the boundary condition for the Euler set on the condensing boundary. Therefore, the analysis of the half-space problem in Refs. 24 and 25 gives important information also in practical point of view. However, these references deal exclusively with the case where the vapor flow is condensing on the condensed phase perpendicularly. In order to obtain the boundary condition for the Euler set for the general geometry, we need to extend the results of Refs. 24 and 25 to the case where the vapor is condensing onto the condensed phase at incidence.

For this reason, in the present study, we consider a uniform vapor flow in a half-space condensing onto a plane condensed phase at incidence in the presence of a noncondensable gas. We are going to investigate the problem numerically on the basis of kinetic theory, following Ref. 24. In this reference, the case where the molecules of the noncondensable gas are mechanically identical with those of the vapor is considered. In this case, as discussed in Ref. 24, we can successfully decompose the problem into two problems: one is a nonlinear problem for the total mixture and the other is a linear and homogeneous problem for the noncondensable gas. In particular, since the former problem is equivalent to the half-space problem of strong condensation for a pure vapor, we can exploit the rich knowledge and resources accumulated so far. In addition, this decomposition not only reduces the necessary amount of computation dramatically, but also provides a clear understanding of the features of the solution. This situation is the same in the present problem where the vapor is condensing obliquely.

In the present paper, therefore, we consider the same situation in which the molecules of the noncondensable gas are mechanically identical with those of the vapor. Furthermore, as in Refs. 24 and 25, we employ a model Boltzmann equation for a gas mixture proposed by Garzó, Santos, and Brey [the Garzó–Santos–Brey (GSB) model],[34] rather than the original Boltzmann equation, in the actual numerical computation. In this paper (I), we consider the case in which the speed of condensation is subsonic, more precisely, the case where the Mach number based on the component of the flow velocity of the vapor at infinity normal to the boundary is less than unity. The case in which the speed of condensation is supersonic will be considered in the forthcoming paper.

II. FORMULATION OF THE PROBLEM

A. Problem

Consider a vapor in a half space $X_1>0$ bounded by a stationary plane condensed phase of the vapor located at $X_1=0$, where X_i is a rectangular coordinate system. There is a uniform vapor flow at infinity toward the condensed phase with velocity $(v_{\infty 1}, v_{\infty 2}, 0)$ $(v_{\infty 1}<0,\ v_{\infty 2}\geqslant 0)$, temperature T_∞, and pressure p_∞ (or molecular number density $n_\infty = p_\infty/kT_\infty$, where k is the Boltzmann constant). The condensed phase is kept at a constant and uniform temperature T_w. Steady condensation of the vapor is taking place on the condensed phase, and another gas neither condensing nor evaporating on the condensed phase, which we call the noncondensable gas, is confined near the condensed phase by the condensing vapor flow. (See Fig. 1.) We investigate the steady behavior of the vapor and the noncondensable gas on the basis of kinetic theory, under the following assumptions: (i) the behavior of the vapor and the noncondensable gas is described by the Boltzmann equation for a binary mixture (the GSB model[34] will be employed for numerical computation); (ii) the vapor molecules leaving the condensed phase are distributed according to (the part corresponding to the leaving molecules of) the Maxwellian distribution describing the saturated equilibrium state at rest at temperature T_w; (iii) the noncondensable-gas molecules leaving the condensed phase are distributed according to (the part corresponding to

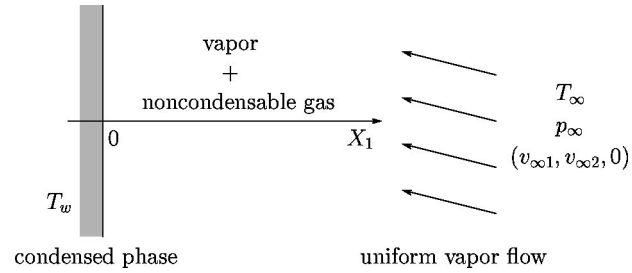

FIG. 1. Uniform flow of a vapor condensing onto its plane condensed phase at incidence in the presence of a noncondensable gas.

the leaving molecules of) the Maxwellian distribution with temperature T_w and flow velocity 0, and there is no net particle flow across the condensed phase (diffuse reflection); (iv) the molecules of the noncondensable gas are mechanically identical with those of the vapor (this assumption, which will be introduced in Sec. III, is not used in the formulation of the problem in Sec. II).

For later use, we introduce the following notation: p_w is the saturated pressure of the vapor at temperature T_w, and n_w is the corresponding molecular number density ($n_w = p_w/kT_w$). In the following, we assign the label A to the vapor (it will also be called A component) and B to the noncondensable gas (it will also be called B component).

B. Basic equation

We first introduce the basic notations: ξ_i is the molecular velocity, F^α the velocity distribution function of the α component ($\alpha=A$ corresponds to the vapor and $\alpha=B$ to the noncondensable gas); n^α is the molecular number density, ρ^α the mass density, T^α the *temperature*, p^α the *pressure*, and $v_i^\alpha=(v_1^\alpha, v_2^\alpha, 0)$ the flow velocity of the α component; n is the molecular number density, ρ the mass density, T the temperature, p the pressure, and $v_i=(v_1, v_2, 0)$ the flow velocity of the total mixture; m^α is the mass of a molecule of the α component. Then we introduce the dimensionless variables (x_i, ζ_i, $\hat{F}^\alpha$, $\hat{n}^\alpha$, $\hat{\rho}^\alpha$, $\hat{T}^\alpha$, $\hat{p}^\alpha$, $\hat{v}_i^\alpha$, $\hat{n}$, $\hat{\rho}$, $\hat{T}$, $\hat{p}$, $\hat{v}_i$) corresponding to (X_i, ξ_i, F^α, n^α, ρ^α, T^α, p^α, v_i^α, n, ρ, T, p, v_i) by the following relations:

$$x_i=\frac{X_i}{(\sqrt{\pi}/2)l_\infty}, \quad \zeta_i=\frac{\xi_i}{(2kT_\infty/m^A)^{1/2}}, \tag{1a}$$

$$\hat{F}^\alpha=\frac{(2kT_\infty/m^A)^{3/2}}{n_\infty}F^\alpha, \tag{1b}$$

$$\hat{n}^\alpha=\frac{n^\alpha}{n_\infty}, \quad \hat{\rho}^\alpha=\frac{\rho^\alpha}{m^A n_\infty}, \quad \hat{T}^\alpha=\frac{T^\alpha}{T_\infty}, \tag{1c}$$

$$\hat{p}^\alpha=\frac{p^\alpha}{p_\infty}, \quad \hat{v}_i^\alpha=\frac{v_i^\alpha}{(2kT_\infty/m^A)^{1/2}}, \tag{1d}$$

$$\hat{n}=\frac{n}{n_\infty}, \quad \hat{\rho}=\frac{\rho}{m^A n_\infty}, \quad \hat{T}=\frac{T}{T_\infty}, \tag{1e}$$

$$\hat{p}=\frac{p}{p_\infty}, \quad \hat{v}_i=\frac{v_i}{(2kT_\infty/m^A)^{1/2}}. \tag{1f}$$

Here, l_∞ is the mean free path of the vapor molecules in the equilibrium state at rest with temperature T_∞ and pressure p_∞ (see Appendix A); for example, $l_\infty=[\sqrt{2}\pi(d^A)^2 n_\infty]^{-1}$ for hard-sphere molecules, where d^A is the diameter of a vapor molecule [Eq. (A9b)], and $l_\infty=(2/\sqrt{\pi})(2kT_\infty/m^A)^{1/2}/K^{AA}n_\infty$ for the GSB model, where K^{AA} is a constant (see Appendix B).

Then, the Boltzmann equation for a binary mixture in the present steady and spatially one-dimensional problem is written as

$$\zeta_1\frac{\partial \hat{F}^\alpha}{\partial x_1}=\sum_{\beta=A,B}\hat{J}^{\beta\alpha}(\hat{F}^\beta,\hat{F}^\alpha) \quad (\alpha=A,B), \tag{2}$$

where $\hat{J}^{\beta\alpha}(\hat{F}^\beta,\hat{F}^\alpha)$ is the dimensionless form of the collision term that expresses the effect of molecular collisions between molecules of the α and β components on the change of $\hat{F}^\alpha$. Its explicit form is given in Appendix A [Eq. (A1)].

The boundary condition on the condensed phase is given by

$$\hat{F}^A=\pi^{-3/2}\frac{n_w}{n_\infty}\left(\frac{T_\infty}{T_w}\right)^{3/2}\exp\left(-\frac{T_\infty}{T_w}\zeta_i^2\right), \tag{3a}$$

$$\hat{F}^B=\pi^{-3/2}\frac{\sigma_w^B}{n_\infty}\left(\frac{m^B}{m^A}\right)^{3/2}\left(\frac{T_\infty}{T_w}\right)^{3/2}\exp\left(-\frac{m^B}{m^A}\frac{T_\infty}{T_w}\zeta_i^2\right), \tag{3b}$$

$$\text{for } \zeta_1>0, \text{ at } x_1=0,$$

where

$$\frac{\sigma_w^B}{n_\infty}=-2\sqrt{\pi}\left(\frac{m^B}{m^A}\right)^{1/2}\left(\frac{T_\infty}{T_w}\right)^{1/2}\int_{\zeta_1<0}\zeta_1\hat{F}^B\,d^3\zeta, \tag{4}$$

with $d^3\zeta=d\zeta_1\,d\zeta_2\,d\zeta_3$. The condition at infinity is

$$\hat{F}^A\to\pi^{-3/2}\exp\left(-\left(\zeta_i-\frac{v_{\infty i}}{\sqrt{2kT_\infty/m^A}}\right)^2\right), \tag{5a}$$

$$\hat{F}^B\to 0, \tag{5b}$$

$$\text{as } x_1\to\infty,$$

where $v_{\infty i}=(v_{\infty 1}, v_{\infty 2}, 0)$. For convenience of the later use, we introduce the normal and tangential Mach numbers $M_{n\infty}$ (>0) and $M_{t\infty}$ ($\geqslant 0$) at infinity,

$$M_{n\infty}=\frac{-v_{\infty 1}}{\sqrt{5kT_\infty/3m^A}}, \quad M_{t\infty}=\frac{v_{\infty 2}}{\sqrt{5kT_\infty/3m^A}}. \tag{6}$$

Then, the dimensionless velocity $v_{\infty i}/\sqrt{2kT_\infty/m^A}$ in Eq. (5a) is written as

$$\frac{v_{\infty i}}{\sqrt{2kT_\infty/m^A}}=\sqrt{\frac{5}{6}}(-M_{n\infty},\ M_{t\infty},\ 0). \tag{7}$$

Here, we have given the basic equations and boundary conditions in a dimensionless form. The corresponding dimensional form is readily obtained by the use of Eqs. (1a)–(1f) and the relations relevant to the collision integrals summarized in Appendix A.

As is seen from Eqs. (2)–(7), the parameters imposed externally, that is, T_w, n_w, T_∞, n_∞, $v_{\infty 1}$, and $v_{\infty 2}$, appear as the following set:

$$M_{n\infty}, \quad M_{t\infty}, \quad \frac{T_\infty}{T_w}, \quad \frac{n_\infty}{n_w}\left(\text{or } \frac{p_\infty}{p_w}\right), \tag{8}$$

in the nondimensionalized boundary-value problem [note that Eq. (2) does not contain these parameters]. On the other hand, it is physically obvious that we need to specify a parameter related to the amount of the noncondensable gas to single out a solution. In Ref. 24, the following Γ is used as this parameter:

$$\Gamma = \frac{2}{\sqrt{\pi}} \frac{1}{n_\infty l_\infty} \int_0^\infty n^B \, dX_1 = \int_0^\infty \hat{n}^B \, dx_1. \tag{9}$$

It corresponds to the total number of molecules of the noncondensable gas per unit area of the condensed phase.

C. Macroscopic quantities

The macroscopic quantities $\hat{n}^\alpha$, $\hat{\rho}^\alpha$, $\hat{v}_i^\alpha$, $\hat{p}^\alpha$, $\hat{T}^\alpha$, $\hat{n}$, $\hat{\rho}$, $\hat{v}_i$, $\hat{p}$, and $\hat{T}$ are defined as follows:

$$\hat{n}^\alpha = \int \hat{F}^\alpha \, d^3\zeta, \quad \hat{\rho}^\alpha = \hat{m}^\alpha \hat{n}^\alpha, \tag{10a}$$

$$\hat{v}_i^\alpha = \frac{1}{\hat{n}^\alpha} \int \zeta_i \hat{F}^\alpha \, d^3\zeta, \tag{10b}$$

$$\hat{p}^\alpha = \hat{n}^\alpha \hat{T}^\alpha = \frac{2}{3} \hat{m}^\alpha \int (\zeta_i - \hat{v}_i^\alpha)^2 \hat{F}^\alpha \, d^3\zeta, \tag{10c}$$

$$\hat{n} = \int \sum_{\beta=A,B} \hat{F}^\beta \, d^3\zeta, \quad \hat{\rho} = \int \sum_{\beta=A,B} \hat{m}^\beta \hat{F}^\beta \, d^3\zeta, \tag{10d}$$

$$\hat{v}_i = \frac{1}{\hat{\rho}} \int \zeta_i \sum_{\beta=A,B} \hat{m}^\beta \hat{F}^\beta \, d^3\zeta, \tag{10e}$$

$$\hat{p} = \hat{n}\hat{T} = \frac{2}{3} \int (\zeta_i - \hat{v}_i)^2 \sum_{\beta=A,B} \hat{m}^\beta \hat{F}^\beta \, d^3\zeta, \tag{10f}$$

where $\hat{m}^A = 1$ and $\hat{m}^B = m^B/m^A$. The domain of integration of the integrals with respect to ζ_i in Eqs. (10a)–(10f) is the whole space of ζ_i. The same rule applies to all the integrals with respect to ζ_i in this paper unless the contrary is stated. The macroscopic quantities for the total mixture are expressed in terms of those for individual components as

$$\hat{n} = \sum_{\beta=A,B} \hat{n}^\beta, \quad \hat{\rho} = \sum_{\beta=A,B} \hat{\rho}^\beta, \quad \hat{\rho}\hat{v}_i = \sum_{\beta=A,B} \hat{\rho}^\beta \hat{v}_i^\beta, \tag{11a}$$

$$\hat{p} = \sum_{\beta=A,B} \left[\hat{p}^\beta + \frac{2}{3} \hat{\rho}^\beta (\hat{v}_i^\beta - \hat{v}_i)^2 \right]. \tag{11b}$$

It should be noted that in the literature, the pressure $\hat{p}^\alpha$ and temperature $\hat{T}^\alpha$ of each component are often defined in a different way, i.e., by Eq. (10c) with $\hat{v}_i^\alpha$ replaced by $\hat{v}_i$ of Eq. (10e). Then, the pressure $\hat{p}$ of the total mixture becomes the simple sum of $\hat{p}^A$ and $\hat{p}^B$ rather than Eq. (11b).

The integration of Eq. (2) over the whole ζ_i space leads to $\hat{n}^\alpha \hat{v}_1^\alpha = \text{const}$ because the right-hand side vanishes in the integration. For the noncondensable gas, $\hat{n}^B \hat{v}_1^B = 0$ holds on the condensed phase because of the diffuse reflection (3b) and (4) or at infinity because of Eq. (5b). Therefore, $\hat{n}^B \hat{v}_1^B = 0$ or $\hat{v}_1^B = 0$ holds identically for $x_1 \geqslant 0$.

III. MECHANICALLY IDENTICAL MOLECULES

Following Ref. 24, we now introduce the assumption that the molecules of the vapor and those of the noncondensable gas are mechanically identical. Then, we have

$$m^A = m^B \quad (\text{or } \hat{m}^\alpha = 1), \tag{12a}$$

$$\hat{J}^{\beta\alpha}(\hat{F}^\beta, \hat{F}^\alpha) = \hat{J}(\hat{F}^\beta, \hat{F}^\alpha), \tag{12b}$$

where $\alpha, \beta = A, B$, and $\hat{J}$ is given in Eq. (A10). The discussion in this section is essentially the same as that given in Ref. 24. The only difference is that the case $v_{\infty 2} = 0$ (or $M_{t\infty} = 0$) is considered there. But, we will repeat it for the reader's convenience. The words such as the unique solution will be used in the physical sense, not in the rigorous mathematical sense.

A. Preliminary transformation

Let $\hat{F}$ be the (dimensionless) velocity distribution function of the total mixture defined by

$$\hat{F} = \hat{F}^A + \hat{F}^B. \tag{13}$$

Then, we can transform the boundary-value problem (2)–(5b) for $(\hat{F}^A, \hat{F}^B)$ to the problem for $(\hat{F}, \hat{F}^B)$, which is summarized as follows: the equations are

$$\zeta_1 \frac{\partial \hat{F}}{\partial x_1} = \hat{J}(\hat{F}, \hat{F}), \tag{14a}$$

$$\zeta_1 \frac{\partial \hat{F}^B}{\partial x_1} = \hat{J}(\hat{F}, \hat{F}^B), \tag{14b}$$

the boundary conditions on the condensed phase are

$$\hat{F} = \pi^{-3/2} \frac{n_0}{n_\infty} \left(\frac{T_\infty}{T_w}\right)^{3/2} \exp\left(- \frac{T_\infty}{T_w} \zeta_i^2 \right), \tag{15a}$$

$$\hat{F}^B = \pi^{-3/2} \frac{\sigma_w^B}{n_\infty} \left(\frac{T_\infty}{T_w}\right)^{3/2} \exp\left(- \frac{T_\infty}{T_w} \zeta_i^2 \right), \tag{15b}$$

$$\text{for } \zeta_1 > 0, \text{ at } x_1 = 0,$$

with

$$n_0 = n_w + \sigma_w^B, \tag{16a}$$

$$\frac{\sigma_w^B}{n_\infty} = -2\sqrt{\pi} \left(\frac{T_\infty}{T_w}\right)^{1/2} \int_{\zeta_1 < 0} \zeta_1 \hat{F}^B \, d^3\zeta, \tag{16b}$$

and the conditions at infinity are

$$\hat{F} \to \pi^{-3/2} \exp\left(- \left(\zeta_i - \frac{v_{\infty i}}{\sqrt{2kT_\infty/m^A}} \right)^2 \right), \tag{17a}$$

$$\hat{F}^B \to 0, \quad \text{as } x_1 \to \infty. \tag{17b}$$

Here, Eq. (14a), which is the Boltzmann equation for a single-component gas, is obtained by adding Eq. (2) with $\alpha = A$ and B and by taking into account the bilinearity of $\hat{J}$. Equation (14b) is Eq. (2) (with $\alpha = B$) with $\hat{F}^A$ being eliminated by the use of Eq. (13). Equations (15a) and (17a) are, respectively, the sum of Eqs. (3a) and (3b) and that of Eqs. (5a) and (5b).

B. Half-space problem for a pure vapor

Now, let us suppose that n_0 (or n_0/n_∞) in Eq. (15a) is a given parameter. Then, Eqs. (14a), (15a), and (17a) form a boundary-value problem equivalent to the half-space condensation problem for a pure vapor, namely, Eqs. (2)–(5b) with $\hat{F}^B = 0$, which has been studied comprehensively in Refs. 1, 5–7, 11, and 12; $\hat{F}$ and n_0 correspond, respectively, to the (dimensionless) velocity distribution function of the vapor and to the saturation number density of the vapor at temperature T_w. Then, this problem is characterized by the following set of parameters:

$$M_{n\infty}, \quad M_{t\infty}, \quad \frac{T_\infty}{T_w}, \quad \frac{n_\infty}{n_0}\left(\text{or } \frac{p_\infty}{p_0}\right), \tag{18}$$

where $p_0 = k n_0 T_w$, which corresponds to the saturation vapor pressure at temperature T_w.

According to the references quoted above, there is a solution only when these parameters satisfy the following relation:

$$\frac{p_\infty}{p_0} = F_s\left(M_{n\infty}, M_{t\infty}, \frac{T_\infty}{T_w}\right) \quad (M_{n\infty} < 1), \tag{19a}$$

$$\frac{p_\infty}{p_0} \geqslant F_s\left(1_-, M_{t\infty}, \frac{T_\infty}{T_w}\right) \quad (M_{n\infty} = 1), \tag{19b}$$

$$\frac{p_\infty}{p_0} > F_b\left(M_{n\infty}, M_{t\infty}, \frac{T_\infty}{T_w}\right) \quad (M_{n\infty} > 1). \tag{19c}$$

The functions F_s and F_b have been constructed numerically in Refs. 7 (for $M_{t\infty} = 0$) and 5, using the BGK model. According to these results, F_s and F_b have the following properties. (i) Both functions are weakly dependent on $M_{t\infty}$ and T_∞/T_w. (ii) For any fixed $M_{t\infty}$ and T_∞/T_w, F_s is a monotonically increasing function in $M_{n\infty}$, whereas F_b is a monotonically decreasing function in $M_{n\infty}$. (iii) $F_s(0, 0, 1) = F_s(0_+, M_{t\infty}, T_\infty/T_w) = 1$ and $F_s(1_-, M_{t\infty}, T_\infty/T_w) = F_b(1_+, M_{t\infty}, T_\infty/T_w)$ (see, e.g., Ref. 1).

Equations (19a)–(19c) indicate that in order to obtain a unique solution to Eqs. (14a), (15a), and (17a), one needs to specify three parameters, say $M_{n\infty}$, $M_{t\infty}$, and T_∞/T_w, out of the four parameters in Eq. (18) when $M_{n\infty} < 1$ (subsonic condensation) and all the four parameters satisfying the inequality (19b) or (19c) when $M_{n\infty} \geqslant 1$ (supersonic condensation).

It should be mentioned that F_s (with $M_{t\infty} = 0$) has also been computed for hard-sphere molecules by means of the direct simulation Monte Carlo (DSMC) method[35,36] by Sone and Sasaki.[37] The result is quite close to that for the BGK model.

C. Half-space problem in the presence of a noncondensable gas

Let us suppose that we have obtained the solution $\hat{F}$ corresponding to a given value of n_0 (or the parameter n_0/n_∞). Then, Eqs. (14b), (15b), (16b), and (17b) reduce to a linear and homogeneous boundary-value problem for $\hat{F}^B$. Therefore, a solution multiplied by an arbitrary constant is also a solution. The unique solution is determined by specifying Γ [Eq. (9)]. Let us denote by $\hat{F}^B_*$ and Γ_* the solution and the value of Γ corresponding to the case $\sigma^B_w = n_0$ in Eq. (15b). Since Γ is linear in $\hat{F}^B$ [see Eqs. (9) and (10a)], the solution for an arbitrary Γ is expressed in terms of $\hat{F}^B_*$ and Γ_* as

$$\hat{F}^B = (\Gamma/\Gamma_*)\hat{F}^B_*. \tag{20}$$

Then, Eq. (16b) yields

$$\sigma^B_w = (\Gamma/\Gamma_*) n_0, \tag{21}$$

which together with Eq. (16a) gives the relationship between n_w and n_0 or that between p_w and p_0:

$$n_w = (1 - \Gamma/\Gamma_*) n_0, \tag{22a}$$

$$p_w = (1 - \Gamma/\Gamma_*) p_0. \tag{22b}$$

To summarize, we first obtain a solution $\hat{F}$ to the problem (14a), (15a), and (17a) that corresponds to a given n_0 (or n_0/n_∞). Then we solve the problem (14b), (15b), and (17b) for $\sigma^B_w = n_0$ (or $\sigma^B_w/n_\infty = n_0/n_\infty$) to obtain $\hat{F}^B_*$, from which we compute Γ_* using Eqs. (9) and (10a). Then, for a given Γ, we obtain $\hat{F}^B$ from Eq. (20) and $\hat{F}^A$ from Eq. (13). The $\hat{F}^A$ and $\hat{F}^B$ thus obtained solve the original problem (2)–(5b) with Eqs. (12a) and (12b) for the Γ and the saturation number density n_w given by Eq. (22a). Since n_w is not negative physically, Eq. (22a) yields

$$0 \leqslant \Gamma \leqslant \Gamma_*. \tag{23}$$

That is, Γ_* is the maximum Γ for a given $\hat{F}$.

One might think that the above scheme for the solution is practically inconvenient because specifying the artificial parameter n_∞/n_0 rather than the physically inherent parameter n_∞/n_w of the system seems to be crucial. In the case of subsonic condensation, however, the inconvenience does not arise because the solution $\hat{F}$ and $\hat{F}^B$ can be determined by specifying $M_{n\infty}$, $M_{t\infty}$, T_∞/T_w, and Γ only, that is, we do not need to specify n_∞/n_0 or n_∞/n_w (see Sec. III D). On the other hand, the scheme gives a clear understanding of the relationship among the parameters which admits a solution even in the case of supersonic condensation (see Ref. 24).

D. Existence range of a solution: Subsonic condensation

Now we return to the original problem. In the present paper, we restrict ourselves to the case when $M_{n\infty} < 1$. The

case of $M_{n\infty} \geqslant 1$ will be discussed in the subsequent paper. Then, if we specify $M_{n\infty}$, $M_{t\infty}$, and T_∞/T_w, the solution $\hat{F}$ to Eqs. (14a), (15a), and (17a) is determined together with the value of p_∞/p_0 [Eq. (19a)] or $n_\infty/n_0=(p_\infty/p_0)(T_w/T_\infty)$. We use the inverse of n_∞/n_0 thus obtained for σ_w^B/n_∞ in Eq. (15b) to obtain $\hat{F}_*^B$ and then Γ_* from Eq. (9). The $\hat{F}_*^B$ and Γ_* depend on $M_{n\infty}$, $M_{t\infty}$, and T_∞/T_w through $\hat{F}$ in Eq. (14b) and n_0/n_∞ in Eq. (15b). Thus, we may write explicitly $\Gamma_*(M_{n\infty}, M_{t\infty}, T_\infty/T_w)$. If we eliminate p_0 from Eqs. (19a) and (22b), we obtain the desired relation among the parameters that admits a solution in the present problem, i.e.,

$$p_\infty/p_w=\mathcal{F}_s(M_{n\infty},\ M_{t\infty},\ T_\infty/T_w,\ \Gamma), \tag{24}$$

where

$$\mathcal{F}_s(M_{n\infty},\ M_{t\infty},\ T_\infty/T_w,\ \Gamma) = \left(1-\frac{\Gamma}{\Gamma_*(M_{n\infty},\ M_{t\infty},\ T_\infty/T_w)}\right)^{-1} \times F_s(M_{n\infty},\ M_{t\infty},\ T_\infty/T_w). \tag{25}$$

It should be stressed that the functional form of $\mathcal{F}_s$ with respect to Γ is explicit. If we exploit the comprehensive numerical data for F_s obtained by using the BGK model in Ref. 5, our remaining task is to compute $\hat{F}_*^B$ and Γ_* for various values of the set $(M_{n\infty}, M_{t\infty}, T_\infty/T_w)$, using a model collision term that is consistent with the BGK model. In other words, we can construct the function $\mathcal{F}_s$ of four variables by constructing the function Γ_* of three variables. This fact reduces the amount of necessary computation dramatically.

As described in Sec. I, a steady flow of a vapor around the boundary, consisting of the condensed phase of the vapor, is described by the Euler set of equations in the continuum limit when a small amount of a noncondensable gas is contained in the system. The relation (24), with the numerical data for $\mathcal{F}_s$ given in Sec. IV B, gives the essential part of the boundary condition for the Euler set on the condensing boundary in this situation (when the speed of condensation is subsonic). The reader is referred to Ref. 33 for the details.

IV. NUMERICAL ANALYSIS AND RESULTS

In this section, we carry out actual numerical analysis to obtain $\hat{F}_*^B$ and Γ_*, which gives the solution $\hat{F}^A$ and $\hat{F}^B$ of the original problem. Since the numerical technique is essentially the same as that used in the case of a single-component system in Refs. 7 and 5, where the detailed description of the method is given, we omit it here giving some remarks in Sec. IV A and concentrate on the results of analysis. Information about the accuracy of the computation is given in Appendix C.

A. Some remarks on numerical analysis

As in Refs. 24 and 25, we employ the GSB model[34] for Eq. (2). The model collision term is given in Appendix B. The original Boltzmann equation has the property that, when the molecules of the A component are mechanically identical with those of the B component, the equation for $\hat{F}=\hat{F}^A+\hat{F}^B$ coincides with the Boltzmann equation (14a) for a single-component gas, i.e., the equation in the case where $\hat{F}^A=\hat{F}$ and $\hat{F}^B=0$. Although several model Boltzmann equations have been proposed for gas mixtures,[34,38–40] only the GSB model (and the model in Ref. 40 under some restrictions) satisfies this property. Since it plays an essential role in the present approach, we adopt the GSB model. In addition, Eq. (14a) for this model reduces to the BGK model (Appendix B). Therefore, for the solution $\hat{F}$ to Eqs. (14a), (15a), and (17a) and the function F_s in Eq. (25), we can use the detailed data given in Refs. 7 and 5. We just need to solve the linear system (14b) [with Eq. (B6)], (15b) (with $\sigma_w^B=n_0$), and (17b) numerically to obtain $\hat{F}_*^B$ and the corresponding Γ_*.

We solve this problem by means of a finite-difference method. In both systems, Eqs. (14a), (15a), and (17a) and Eqs. (14b), (15b), and (17b), the model collision terms allow us to eliminate the molecular-velocity variables ζ_2 and ζ_3 from the systems, as in the case of the BGK model for a single-component gas.[41] That is, by multiplying the equations and boundary conditions by 1, ζ_2, and $\zeta_2^2+\zeta_3^2$ and by integrating the respective results over the whole range of ζ_2 and ζ_3, we obtain the equations and boundary conditions of the respective sets $(\mathcal{H}_a, \mathcal{H}_b, \mathcal{H}_c)$ and $(\mathcal{H}_{a*}^B, \mathcal{H}_{b*}^B, \mathcal{H}_{c*}^B)$ of marginal velocity distribution functions defined by

$$(\mathcal{H}_a,\ \mathcal{H}_b,\ \mathcal{H}_c)=\int_{-\infty}^{\infty}\int_{-\infty}^{\infty}(1,\ \zeta_2,\ \zeta_2^2+\zeta_3^2)\hat{F}\,d\zeta_2\,d\zeta_3, \tag{26a}$$

$$(\mathcal{H}_{a*}^B,\ \mathcal{H}_{b*}^B,\ \mathcal{H}_{c*}^B)=\int_{-\infty}^{\infty}\int_{-\infty}^{\infty}(1,\ \zeta_2,\ \zeta_2^2+\zeta_3^2)\times\hat{F}_*^B\,d\zeta_2\,d\zeta_3. \tag{26b}$$

The solution method for the system for $(\mathcal{H}_a, \mathcal{H}_b, \mathcal{H}_c)$ is described in detail in Ref. 5, and that for the system $(\mathcal{H}_{a*}^B, \mathcal{H}_{b*}^B, \mathcal{H}_{c*}^B)$ is essentially the same as the former. Therefore, we avoid the description of the methods for conciseness.

B. Existence range of a solution

In this section, we show some of the numerical results for the existence range of a solution already discussed in Sec. III D, namely the numerical data for the function $\mathcal{F}_s(M_{n\infty}, M_{t\infty}, T_\infty/T_w, \Gamma)$ in Eq. (24). For this purpose, we need to present the data for F_s and Γ_*.

The data for F_s have already been given in Ref. 5. That is, Fig. 3 and Tables I–IV in Ref. 5 show the numerical data of $F_s(M_{n\infty}, M_{t\infty}, T_\infty/T_w)$ for $T_\infty/T_w=0.5$, 1, 1.5, and 2. In the present study, we recomputed all the cases in Ref. 5 and confirmed the accuracy of the data given there. To be more precise, in Tables II–IV of Ref. 5, the last figure should be changed by one in several data, and in Table I there, the last figure should be changed by one in about 20 data for $M_{n\infty} \leqslant 0.9$ and by two to seven in the data for $M_{n\infty}=0.99$. We also made additional computations to supplement these data. Some of the results are shown in Table I, the more comprehensive data being given in Tables I–IV in Ref. 42. The numerical results for $\Gamma_*(M_{n\infty}, M_{t\infty}, T_\infty/T_w)$ obtained in

TABLE I. $F_s(M_{n\infty}, M_{t\infty}, T_\infty/T_w)$ as a function of $M_{n\infty}$, $M_{t\infty}$, and T_∞/T_w.

	$T_\infty/T_w=0.5$				$T_\infty/T_w=1$			
$M_{n\infty}\backslash M_{t\infty}$	0	1	2	3	0	1	2	3
0.01	1.0205	1.0229	1.0300	1.0418	1.0197	1.0230	1.0330	1.0495
0.1	1.2294	1.2527	1.3220	1.4354	1.2201	1.2522	1.3470	1.5007
0.2	1.5251	1.5744	1.7213	1.9645	1.5025	1.5693	1.7677	2.0941
0.3	1.9126	1.9933	2.2352	2.6375	1.8692	1.9778	2.3021	2.8401
0.4	2.4288	2.5492	2.9104	3.5123	2.3517	2.5127	2.9949	3.7974
0.5	3.1309	3.3023	3.8169	4.6749	2.9965	3.2244	3.9081	5.0475
0.6	4.1102	4.3492	5.0663	6.2621	3.8742	4.1891	5.1344	6.7105
0.7	5.5228	5.8538	6.8472	8.5035	5.0958	5.5262	6.8179	8.9721
0.8	7.6548	8.1168	9.5033	11.815	6.8457	7.4328	9.1951	12.134
0.9	11.096	11.756	13.736	17.039	9.4506	10.258	12.681	16.722
0.95	13.693	14.494	16.898	20.907	11.253	12.205	15.064	19.832
0.99	16.484	17.431	20.271	25.009	13.046	14.139	17.417	22.885
1	17.304	18.292	21.258	26.205	13.549	14.680	18.074	23.734
	$T_\infty/T_w=1.5$				$T_\infty/T_w=2$			
$M_{n\infty}\backslash M_{t\infty}$	0	1	2	3	0	1	2	3
0.01	1.0203	1.0244	1.0366	1.0566	1.0212	1.0259	1.0399	1.0629
0.1	1.2249	1.2636	1.3770	1.5598	1.2328	1.2767	1.4053	1.6117
0.2	1.5106	1.5902	1.8262	2.2131	1.5253	1.6155	1.8820	2.3180
0.3	1.8788	2.0077	2.3924	3.0293	1.9000	2.0457	2.4797	3.1973
0.4	2.3593	2.5499	3.1208	4.0700	2.3864	2.6014	3.2447	4.3138
0.5	2.9950	3.2642	4.0717	5.4170	3.0254	3.3285	4.2375	5.7513
0.6	3.8484	4.2191	5.3315	7.1861	3.8756	4.2920	5.5415	7.6245
0.7	5.0142	5.5174	7.0280	9.5474	5.0229	5.5860	7.2765	10.096
0.8	6.6396	7.3189	9.3583	12.760	6.5955	7.3508	9.6189	13.402
0.9	8.9647	9.8828	12.639	17.236	8.7902	9.8008	12.836	17.898
0.95	10.509	11.579	14.791	20.149	10.212	11.381	14.893	20.752
0.99	11.993	13.205	16.843	22.912	11.552	12.867	16.817	23.407
1	12.401	13.651	17.270	23.666	11.916	13.270	17.337	24.123

the present study are shown in Table II, the more detailed tables being given as Tables V–VIII in Ref. 42.

With these data, we can construct the function $\mathcal{F}_s$. The result for $T_\infty/T_w=1$ is shown in Fig. 2, where $\mathcal{F}_s$ versus $M_{n\infty}$ is shown for various Γ at four values of $M_{t\infty}$, i.e., $M_{t\infty}=0$, 1, 2, and 3. The similar figures for $T_\infty/T_w=0.5$, 1.5, and 2 are given as Figs. 1, 3, and 4 in Ref. 42 (Fig. 2 in Ref. 42 is the same as Fig. 2 here). The $\mathcal{F}_s$ is an increasing function of $M_{n\infty}$, and its curve moves upward with the increase of Γ. The Γ_c in the figures is a critical value of Γ, depending on $M_{t\infty}$ and T_∞/T_w, introduced by Eq. (27) below. When $\Gamma<\Gamma_c$, $\mathcal{F}_s$ takes a finite value at $M_{n\infty}=1$. But, when $\Gamma\geqslant\Gamma_c$, $\mathcal{F}_s$ becomes infinitely large as $M_{n\infty}$ approaches a critical value M_c ($\leqslant 1$) that depends on $M_{t\infty}$, T_∞/T_w, and Γ ($M_c=1$ when $\Gamma=\Gamma_c$). That is, $M_{n\infty}=M_c$ is the asymptote of the curve. Therefore, when $\Gamma>\Gamma_c$, there is no solution in the interval $M_c\leqslant M_{n\infty}<1$. More detailed information about Γ_c and M_c will be given below.

Because the dependence of F_s and Γ_* on $M_{t\infty}$ is not strong, the function $\mathcal{F}_s$ does not depend much on $M_{t\infty}$. Therefore, the features of $\mathcal{F}_s$ are essentially the same as those described in Refs. 24 and 25 for the case of $M_{t\infty}=0$. In particular, for $M_{t\infty}$ smaller than around 1 and $M_{n\infty}$ smaller than around 0.5, $\mathcal{F}_s$ is almost independent of $M_{t\infty}$. The dependence of $\mathcal{F}_s$ on T_∞/T_w is also weak in general (see Figs. 1–4 in Ref. 42). The F_s is an increasing function of $M_{n\infty}$, whereas Γ_* is its decreasing function. Therefore, as is seen from Eq. (25), $\mathcal{F}_s$ is an increasing function of $M_{n\infty}$ (see Fig. 2). Numerical results show that $F_s\to 1$ and $\Gamma_*\to\infty$ as $M_{n\infty}\to 0$, and F_s and Γ_* approach finite values as $M_{n\infty}\to 1$. The values of F_s and Γ_* at $M_{n\infty}=1$ in Tables I and II (and in Tables I–IV and V–VIII in Ref. 42) are the values obtained by extrapolation, in which many additional data that are not included in the tables have also been used. Let us set

$$\Gamma_c\left(M_{t\infty}, \frac{T_\infty}{T_w}\right)=\lim_{M_{n\infty}\to 1}\Gamma_*\left(M_{n\infty}, M_{t\infty}, \frac{T_\infty}{T_w}\right). \tag{27}$$

The properties of $\mathcal{F}_s$ described in the preceding paragraph follow immediately from Eqs. (25) and (27) and the fact that Γ_* is a decreasing function of $M_{n\infty}$. That is, when $\Gamma<\Gamma_c$, the Γ/Γ_* in Eq. (25) is less than unity and thus $\mathcal{F}_s$ remains finite in the whole range of $0<M_{n\infty}<1$. When $\Gamma>\Gamma_c$ (or $\Gamma=\Gamma_c$), the Γ/Γ_* in Eq. (25) becomes unity at an $M_{n\infty}$ (<1) (or at $M_{n\infty}=1$). We denote this value of $M_{n\infty}$ by M_c ($M_c=1$ for $\Gamma=\Gamma_c$). Then, $\mathcal{F}_s$ increases indefinitely as $M_{n\infty}$ approaches M_c. The $\Gamma_c(M_{t\infty}, T_\infty/T_w)$ versus $M_{t\infty}$ is shown in Fig. 3, where Γ_c versus $M_{t\infty}$ is plotted for $T_\infty/T_w=0.5$, 1, 1.5, and 2. The $M_c(M_{t\infty}, T_\infty/T_w, \Gamma)$, which is the solution of

$$\Gamma_*(M_c, M_{t\infty}, T_\infty/T_w)-\Gamma=0, \tag{28}$$

is shown in Fig. 4, where M_c versus $M_{t\infty}$ at $T_\infty/T_w=0.5$, 1,

TABLE II. $\Gamma_*(M_{n\infty}, M_{t\infty}, T_\infty/T_w)$ as a function of $M_{n\infty}$, $M_{t\infty}$, and T_∞/T_w.

	$T_\infty/T_w=0.5$				$T_\infty/T_w=1$			
$M_{n\infty}\backslash M_{t\infty}$	0	1	2	3	0	1	2	3
0.01	106.72	106.70	106.64	106.55	107.51	107.49	107.43	107.33
0.05	19.302	19.246	19.080	18.814	19.923	19.857	19.663	19.353
0.1	8.5549	8.4862	8.2895	7.9896	9.0326	8.9466	8.7033	8.3404
0.2	3.3822	3.3197	3.1492	2.9103	3.6851	3.6013	3.3785	3.0791
0.3	1.7822	1.7344	1.6085	1.4428	1.9850	1.9177	1.7471	1.5349
0.4	1.0496	1.0151	0.927 01	0.816 44	1.1902	1.1398	1.0166	0.872 09
0.5	0.651 74	0.627 82	0.567 87	0.495 17	0.752 04	0.715 70	0.629 26	0.532 33
0.6	0.414 66	0.398 49	0.358 55	0.311 25	0.487 91	0.462 37	0.402 92	0.338 41
0.7	0.265 32	0.254 68	0.228 65	0.198 27	0.319 98	0.302 45	0.262 25	0.219 61
0.8	0.168 01	0.161 25	0.144 78	0.125 69	0.209 67	0.197 93	0.171 26	0.143 35
0.9	0.103 31	0.099 232	0.089 285	0.077 745	0.135 74	0.128 12	0.110 87	0.092 918
0.95	0.079 409	0.076 331	0.068 811	0.060 058	0.108 27	0.102 23	0.088 546	0.074 293
0.99	0.063 353	0.060 950	0.055 061	0.048 175	0.089 791	0.084 822	0.073 549	0.061 788
1	0.059 725	0.057 473	0.051 952	0.045 488	0.085 603	0.080 878	0.070 154	0.058 957
	$T_\infty/T_w=1.5$				$T_\infty/T_w=2$			
$M_{n\infty}\backslash M_{t\infty}$	0	1	2	3	0	1	2	3
0.01	107.87	107.85	107.78	107.68	108.08	108.06	108.00	107.89
0.05	20.213	20.141	19.931	19.597	20.391	20.315	20.093	19.742
0.1	9.2609	9.1647	8.8948	8.4975	9.4019	9.2986	9.0105	8.5902
0.2	3.8333	3.7368	3.4842	3.1529	3.9257	3.8203	3.5475	3.1956
0.3	2.0858	2.0069	1.8108	1.5745	2.1490	2.0619	1.8487	1.5973
0.4	1.2614	1.2013	1.0579	0.895 88	1.3063	1.2393	1.0825	0.909 49
0.5	0.803 92	0.759 77	0.657 86	0.548 27	0.836 99	0.787 32	0.674 99	0.557 41
0.6	0.526 79	0.495 18	0.424 01	0.350 31	0.551 92	0.515 95	0.436 77	0.357 20
0.7	0.349 89	0.327 71	0.278 70	0.229 31	0.369 54	0.343 96	0.288 80	0.235 03
0.8	0.233 24	0.217 99	0.184 70	0.151 74	0.249 02	0.231 13	0.193 12	0.156 82
0.9	0.154 78	0.144 53	0.122 29	0.100 48	0.167 77	0.155 48	0.129 59	0.105 15
0.95	0.125 55	0.117 23	0.099 204	0.081 544	0.137 46	0.127 35	0.106 08	0.086 078
0.99	0.105 87	0.098 873	0.083 702	0.068 840	0.117 04	0.108 42	0.090 305	0.073 281
1	0.101 41	0.094 710	0.080 190	0.065 962	0.112 40	0.104 12	0.086 727	0.070 380

1.5, and 2 is plotted for various values of Γ; M_c is taken as the abscissa for easy comparison with Fig. 2 (and Figs. 1–4 in Ref. 42).

In the present analysis, we have taken full advantage of the case where the molecules of the noncondensable gas are mechanically the same as those of the vapor, and furthermore we have used the GSB model to obtain the numerical results such as shown in Fig. 2. A preliminary numerical analysis of the present problem using the DSMC method has also been carried out for hard-sphere molecules in a more general case where the molecules of the two components are not identical mechanically [Aoki, Takata, and Fujimoto (unpublished)]. The result suggests that the relation of the form (24) with $\mathcal{F}_s$ depending on m^B/m^A and d^B/d^A holds in this case (d^α is the diameter of the molecules of the α component). As an example, $\mathcal{F}_s$ for $m^B/m^A=2$ and $d^B/d^A=1$ is shown in Fig. 5 in the case $M_{t\infty}=0$ and $T_\infty/T_w=1$. The qualitative feature of the figure is the same as that of Fig. 2.

C. Macroscopic quantities

In this section, we give some results for the macroscopic quantities. Figures 6–8 show the profiles of the macroscopic quantities for $T_\infty/T_w=1$ and for three different values of $M_{n\infty}$, i.e., Fig. 6 for $M_{n\infty}=0.1$, Fig. 7 for $M_{n\infty}=0.5$, and Fig. 8 for $M_{n\infty}=0.9$. In each figure, the result for $M_{t\infty}=1$ is shown in (a) and that for $M_{t\infty}=3$ in (b). In these figures, the dimensional quantities listed in the beginning of Sec. II B are used rather than their dimensionless counterparts, and the notation $a_\infty=(5kT_\infty/3m^A)^{1/2}$ has been introduced. It is seen from Eqs. (10a)–(10c) with $\alpha=B$ and with $\hat{v}_1^B=0$ (see the last part of Sec. II C) that $\hat{n}^B$, $\hat{n}^B\hat{v}_2^B$, and $\hat{p}^B=\hat{n}^B\tilde{T}^B$ are linear in $\hat{F}^B$. Therefore, because of the form (20), $(\Gamma_*/\Gamma)\hat{n}^B$, $\hat{v}_2^B$, $\hat{T}^B$, and $(\Gamma_*/\Gamma)\hat{p}^B$, i.e., $(\Gamma_*/\Gamma)(n^B/n_\infty)$, $v_2^B/(2kT_\infty/m^A)^{1/2}$, T^B/T_∞, and $(\Gamma_*/\Gamma)(p^B/p_\infty)$, are independent of Γ. It should be noted that n, v_1, v_2, T, and p of the total mixture are the same as n^A, v_1^A, v_2^A, T^A, and p^A for $\Gamma=0$, respectively.

The noncondensable gas extends far away when $M_{n\infty}$ is small (over $50l_\infty$ when $M_{n\infty}=0.1$; see Fig. 6) but is confined in a narrower region when $M_{n\infty}$ is large. For large $M_{t\infty}$, the temperature near the condensed phase increases because of the strong friction. But the temperature rise is smaller for larger $M_{n\infty}$ because the heated gas near the condensed phase is removed by the strong condensation. These features are the same as those discussed in Refs. 5 (for $\Gamma=0$) and 24 (for $M_{t\infty}=0$). The acceleration of the vapor toward the condensed phase is larger for larger Γ because p_w/p_∞ is smaller, i.e., the suction effect on the condensed phase is stronger. As discussed in Ref. 24, because of $v_1^B=0$, F^B does not accommodate to F^A, which is close to the equilibrium distribution

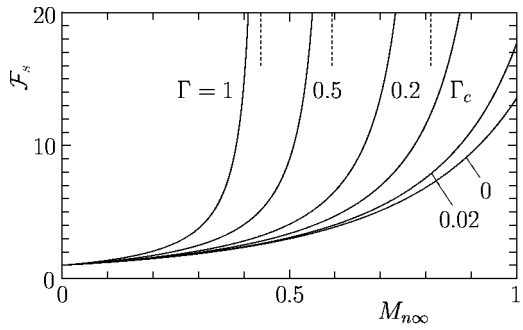

(a) $M_{t\infty} = 0$

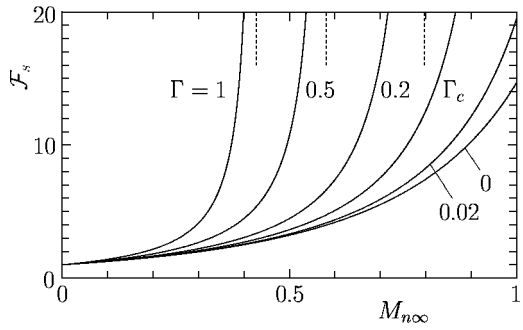

(b) $M_{t\infty} = 1$

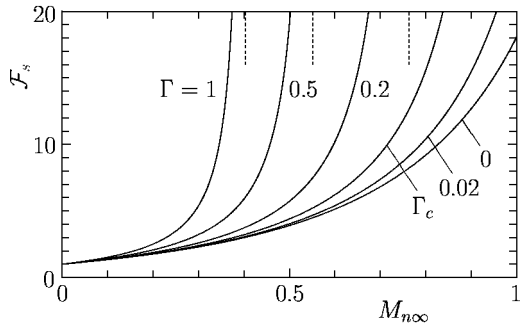

(c) $M_{t\infty} = 2$

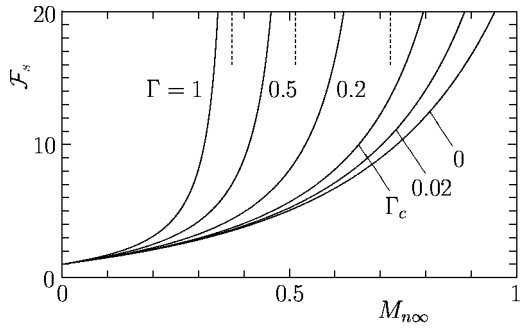

(d) $M_{t\infty} = 3$

FIG. 2. $\mathcal{F}_s(M_{n\infty}, M_{t\infty}, T_\infty/T_w, \Gamma)$ versus $M_{n\infty}$ for various Γ and $M_{t\infty}$ ($T_\infty/T_w = 1$). (a) $M_{t\infty} = 0$, (b) $M_{t\infty} = 1$, (c) $M_{t\infty} = 2$, (d) $M_{t\infty} = 3$. The dotted lines in the figures indicate the asymptotes ($M_{n\infty} = M_c$) of the curves for $\Gamma = 0.2$, 0.5, and 1. The value of Γ_c in each figure is as follows: (a) 0.059 725, (b) 0.057 473, (c) 0.051 952, (d) 0.045 488.

with velocity ($v_{\infty 1}$, $v_{\infty 2}$, 0), even in the far field where n^B is small. In consequence, v_2^B and T^B do not approach $v_{\infty 2}$ and T_∞, respectively (the gradients of these quantities may not vanish at infinity; see Ref. 24).

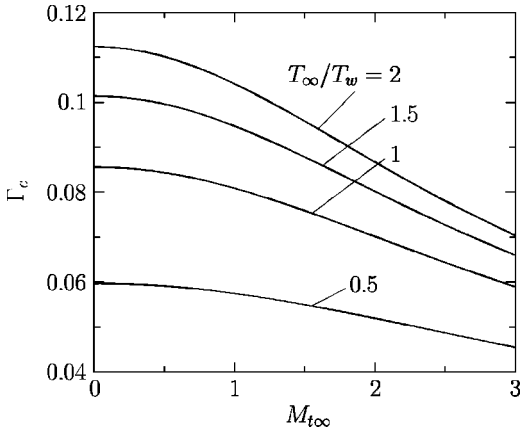

FIG. 3. Γ_c versus $M_{t\infty}$ for $T_\infty/T_w = 0.5$, 1, 1.5, and 2.

As is seen from Figs. 6–8, there is a macroscopic motion of the noncondensable gas along the condensed phase (i.e., in the X_2 direction) when the vapor flow at infinity has a transversal component (i.e., $v_{\infty 2} > 0$). Let us denote by $\mathcal{N}_f$ the dimensional total particle flux (per unit width in X_3 and per unit time) of the noncondensable gas in the X_2 direction and by $\hat{\mathcal{N}}_f$ its dimensionless counterpart defined by

$$\hat{\mathcal{N}}_f = (2/\sqrt{\pi})[n_\infty l_\infty (2kT_\infty/m^A)^{1/2}]^{-1}\mathcal{N}_f. \tag{29}$$

Then, $\hat{\mathcal{N}}_f$ is expressed as

$$\hat{\mathcal{N}}_f = \int_0^\infty \hat{n}^B \hat{v}_2^B \, dx_1 = \int_0^\infty \left(\int \zeta_2 \hat{F}^B \, d^3\zeta \right) dx_1. \tag{30}$$

If we use Eq. (20) in Eq. (30) and denote by $\hat{\mathcal{N}}_{f*}$ the $\hat{\mathcal{N}}_f$ corresponding to $\hat{F}_*^B$, then we have

$$\hat{\mathcal{N}}_f = (\Gamma/\Gamma_*)\hat{\mathcal{N}}_{f*}. \tag{31}$$

We recall that $\hat{F}_*^B$ depends on $M_{n\infty}$, $M_{t\infty}$, and T_∞/T_w, so that $\hat{\mathcal{N}}_{f*}$, as well as Γ_*, is a function of these three parameters. Therefore, setting $\mathcal{G} = \hat{\mathcal{N}}_{f*}/\Gamma_*$, we can write

$$\hat{\mathcal{N}}_f = \Gamma \mathcal{G}(M_{n\infty}, \ M_{t\infty}, \ T_\infty/T_w). \tag{32}$$

The relation (32), or more generally, the $\hat{\mathcal{N}}_f$ as the function of $M_{n\infty}$, $M_{t\infty}$, T_∞/T_w, and Γ, is required as a part of the boundary condition for the Euler set in the continuum limit in the situation described in Sec. I and in the end of Sec. III D (see Ref. 33 for the details). Some of the numerical results for $\mathcal{G}$ are given in Fig. 9, where $\mathcal{G}$ versus $M_{n\infty}$ is plotted for typical $M_{t\infty}$ and T_∞/T_w, and in Table III (see Tables IX–XII in Ref. 42 for more detailed data). The values of $\mathcal{G}$ at $M_{n\infty} = 1$ in Table III (and in Tables IX–XII in Ref. 42) are those obtained by extrapolation using the data for $M_{n\infty} < 1$ in the tables and many additional data not shown there. As is seen from Fig. 9 and the tables, $\mathcal{G}$ is almost linear in $M_{t\infty}$ and weakly dependent on $M_{n\infty}$.

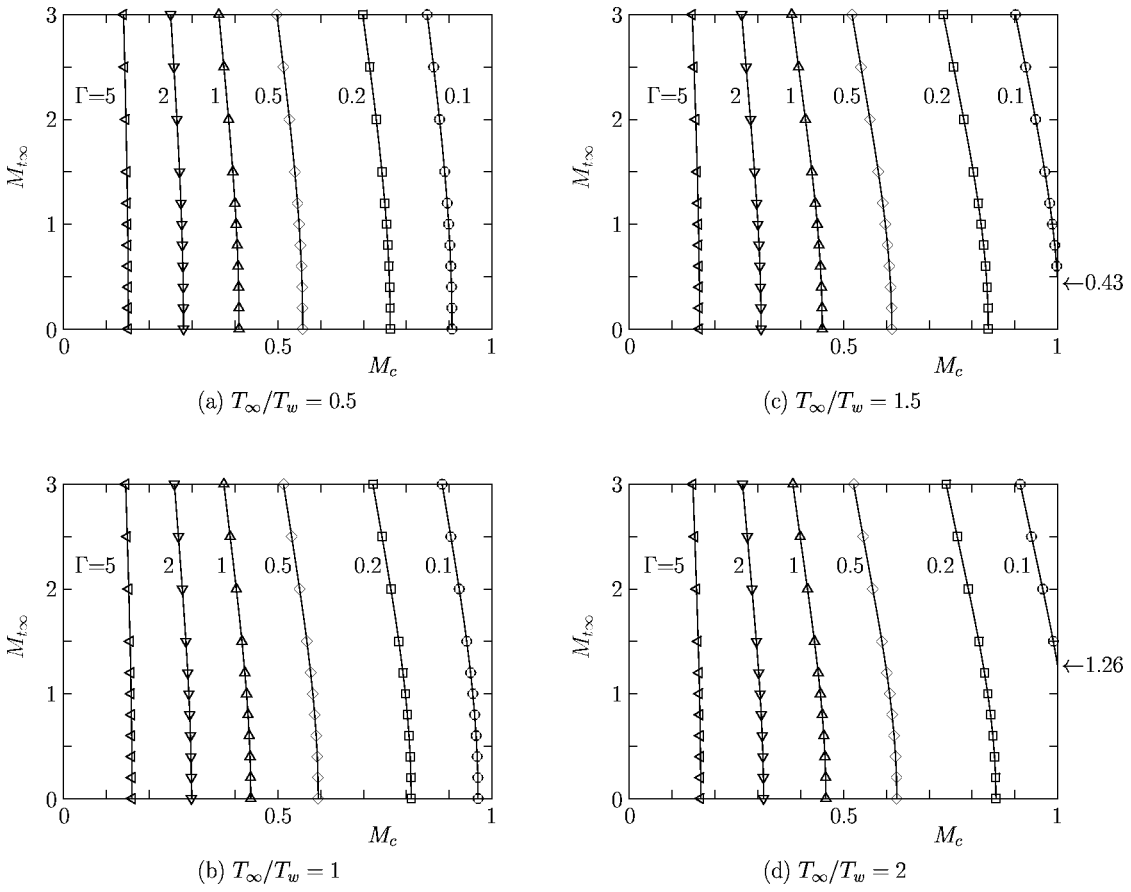

FIG. 4. M_c versus $M_{t\infty}$ for various Γ. (a) $T_\infty/T_w=0.5$, (b) $T_\infty/T_w=1$, (c) $T_\infty/T_w=1.5$, (d) $T_\infty/T_w=2$. M_c is taken as the abscissa for easy comparison with Fig. 2 (and Figs. 1–4 in Ref. 42). In (c) and (d), the curve for $\Gamma=0.1$ intersects $M_c=1$ at $M_{t\infty}=0.43$ and 1.26, respectively.

V. COMMENT ON THE CASE OF EVAPORATION

In this paper, we have exclusively considered the case of condensation, $v_{\infty 1}<0$. Here, we give a short comment on the case of evaporation, i.e., the boundary-value problem (2)–(5b) with $v_{\infty 1}>0$.

Let us first consider the following time-dependent half-space problem: there is a steady flow of a vapor evaporating from the plane condensed phase and flowing toward infinity; we inject an amount of a noncondensable gas suddenly near the condensed phase and pursue the time evolution in the half-space. It is intuitively obvious that the evaporating vapor flow sweeps away the noncondensable gas to infinity, and the latter gas disappears in the long-time limit. This suggests that the steady boundary-value problem, Eqs. (2)–(5b), should have the solution $\hat{F}^B=0$ uniquely when $v_{\infty 1}>0$. Thus, the problem is reduced to that of evaporation of a pure vapor. On the other hand, this conclusion is not obvious mathematically from the equation and boundary conditions. However, if we consider the case of Maxwellian molecules for both components (i.e., the case where the intermolecular force is proportional to r^{-5} with r being the distance between two molecules) or the GSB model, it can be shown easily.

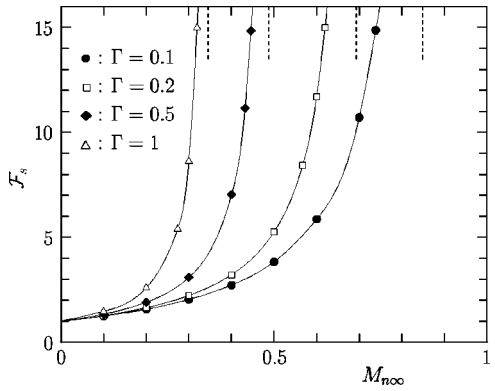

FIG. 5. DSMC result of $\mathcal{F}_s$ for hard-sphere molecules. The $\mathcal{F}_s$ versus $M_{n\infty}$ is shown in the case $m^B/m^A=2$ and $d^B/d^A=1$ ($M_{t\infty}=0$ and $T_\infty/T_w=1$). The dotted lines in the figure indicate the asymptotes of the curves for $\Gamma=0.1$, 0.2, 0.5, and 1. The symbols ●, □, ◆, and △ indicate the numerical data, which are connected by spline curves.

Let us consider Eq. (2) with $\alpha=B$. Integrating the equation multiplied by ζ_1 over the whole space of ζ_i yields

$$\frac{\partial}{\partial x_1}\int \zeta_1^2 \hat{F}^B\, d^3\zeta = \int \zeta_1 \hat{J}^{AB}(\hat{F}^A,\ \hat{F}^B) d^3\zeta, \tag{33}$$

because $\hat{J}^{BB}(\hat{F}^B, \hat{F}^B)$ vanishes in the integration. For Maxwellian molecules, the right-hand side of Eq. (33) can be expressed in terms of the macroscopic quantities as (see, for example, Refs. 34, 40, and 45)

$$\int \zeta_1 \hat{J}^{AB}(\hat{F}^A,\ \hat{F}^B) d^3\zeta = \kappa^{AB}\hat{n}^A\hat{n}^B(\hat{v}_1^A-\hat{v}_1^B), \tag{34}$$

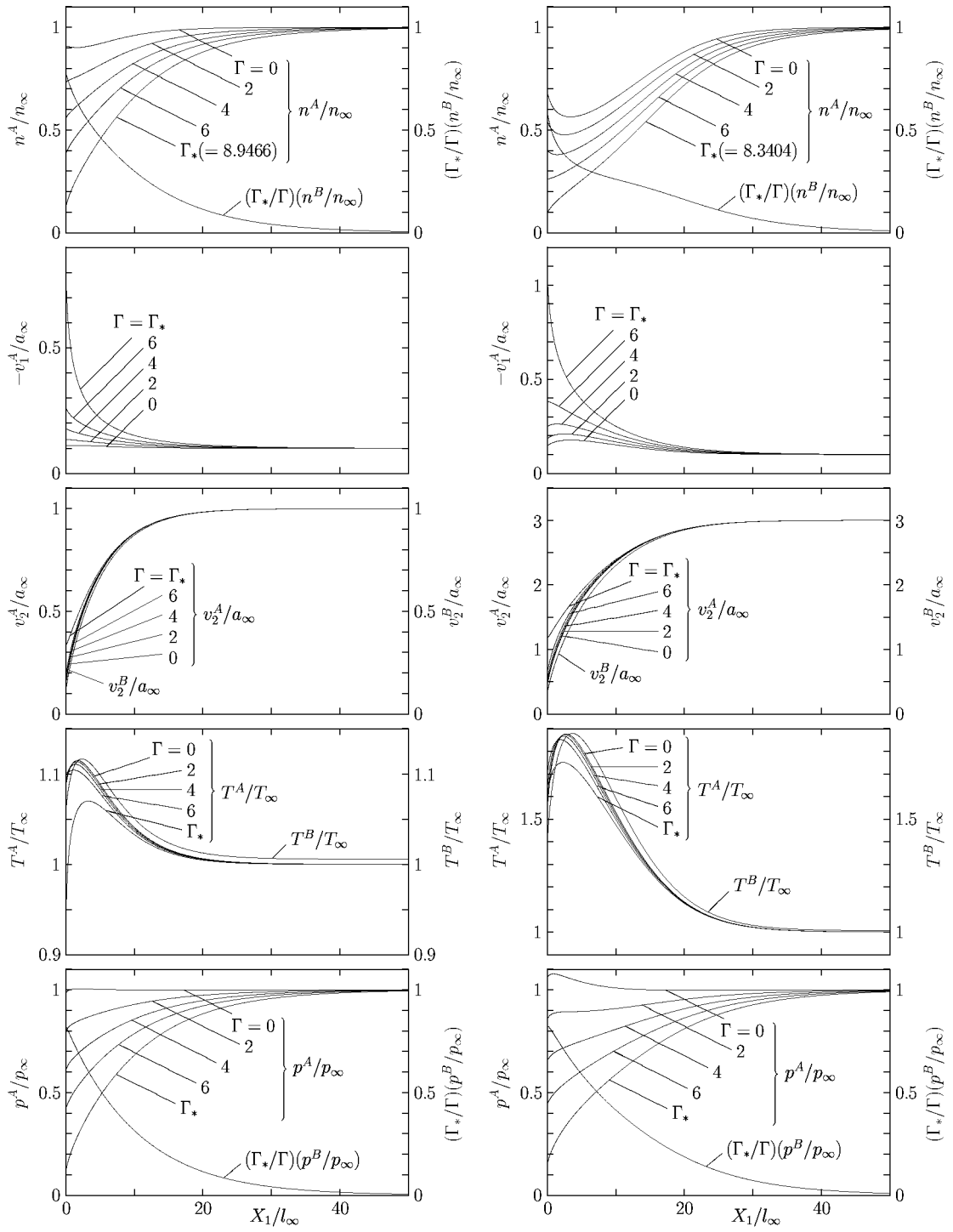

FIG. 6. Profiles of the macroscopic quantities for $M_{n\infty}=0.1$ and $T_\infty/T_w=1$. (a) $M_{t\infty}=1$, (b) $M_{t\infty}=3$. Here, $a_\infty=(5kT_\infty/3m^A)^{1/2}$ is the sound speed at temperature T_∞. The macroscopic quantities of the total mixture are given by those of the vapor for $\Gamma=0$. The profiles of $(\Gamma_*/\Gamma)(n^B/n_\infty)$, v_2^B/a_∞, T^B/T_∞, and $(\Gamma_*/\Gamma)(p^B/p_\infty)$ are independent of Γ.

where κ^{AB} is a positive constant depending on the constant in the intermolecular force law and on $\hat{\mu}^{AB}$ defined in Eq. (A2b). Since $\hat{v}_1^A>0$ and $\hat{n}^B\hat{v}_1^B=0$ (see the last part of Sec. II C), the right-hand side of Eq. (33) is strictly positive. Therefore, $\int\zeta_1^2\hat{F}^B d^3\zeta\geqslant 0$ is a monotonically increasing function of x_1. On the other hand, it should vanish at infinity because of the condition (5b). This is possible only when $\hat{F}^B$ is identically zero.

Most of the model equations for multicomponent mixtures, such as proposed in Refs. 34, 38–40, are designed in such a way that the model collision terms reproduce the momentum and energy transport between different species for Maxwellian molecules. Therefore, they satisfy the relation (34) with an appropriate constant corresponding to κ^{AB}. Thus, $\hat{F}^B=0$ is also true for these model equations.

In connection with the above conclusion, it should be

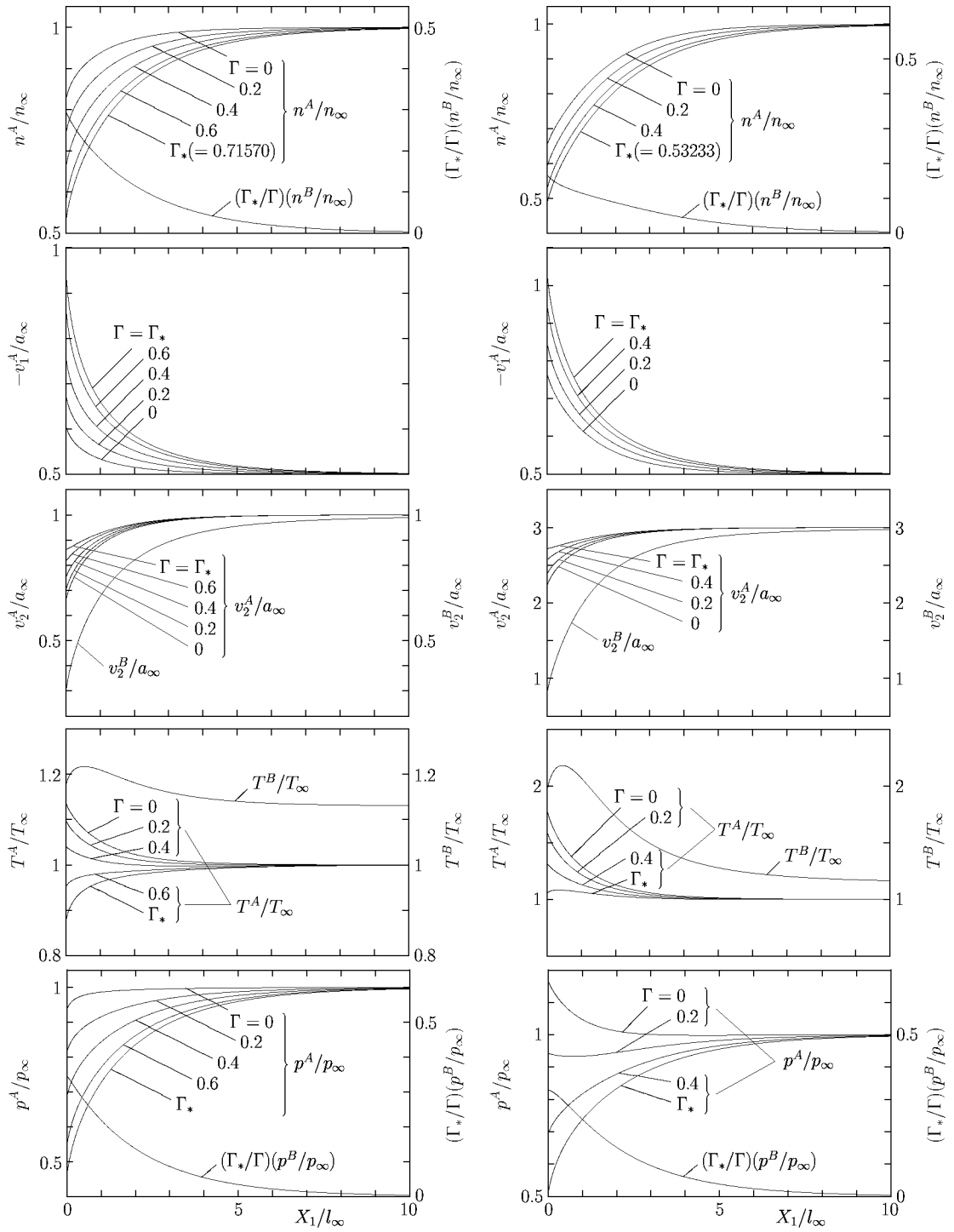

FIG. 7. Profiles of the macroscopic quantities for $M_{n\infty}=0.5$ and $T_\infty/T_w=1$. (a) $M_{t\infty}=1$, (b) $M_{t\infty}=3$. See the caption of Fig. 6.

mentioned that unsteady evaporation into a half-space initially filled with a uniform noncondensable gas is investigated numerically using the GSB model in Refs. 43 and 44. It is demonstrated that, if the initial number density of the noncondensable gas is smaller than the saturation number density of the vapor corresponding to the wall temperature, all the noncondensable gas is swept away to infinity by the vapor, and the final steady state is the pure-vapor evaporation, i.e., the solution to Eqs. (2)–(5b) with $\hat{F}^B=0$. It is also demonstrated that, if the initial number density of the noncondensable gas is larger than the saturation number density of the vapor, the evaporation stops finally, and the mixture approaches an equilibrium state at rest in the entire half-space.

VI. CONCLUDING REMARKS

In this paper, we have considered a flow of a vapor condensing onto a plane condensed phase of the vapor at inci-

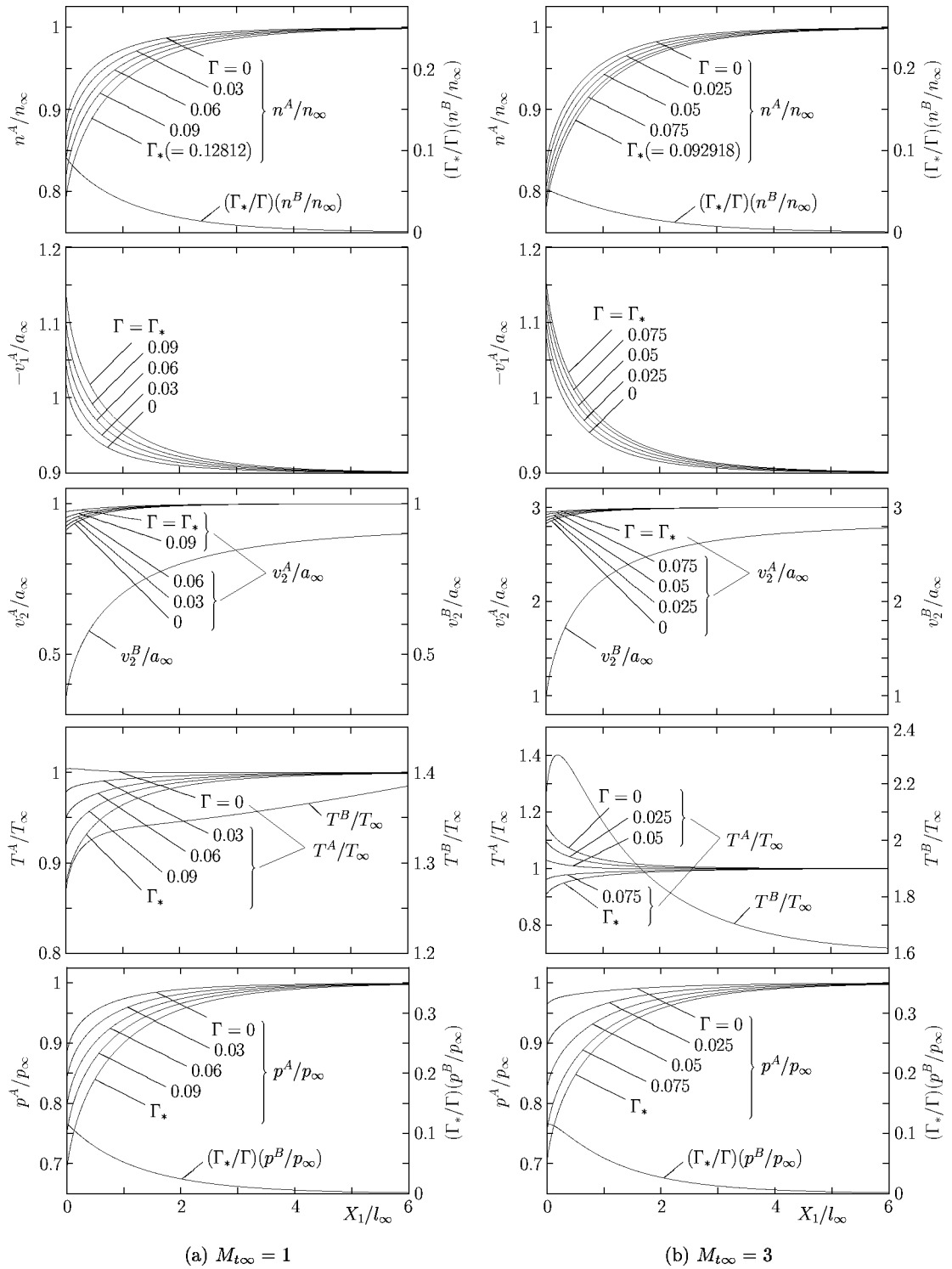

(a) $M_{t\infty} = 1$ (b) $M_{t\infty} = 3$

FIG. 8. Profiles of the macroscopic quantities for $M_{n\infty}=0.9$ and $T_\infty/T_w=1$. (a) $M_{t\infty}=1$, (b) $M_{t\infty}=3$. See the caption of Fig. 6.

dence in the case where a noncondensable gas is present near the condensed phase. The present study is a continuation of Ref. 24, where the vapor is assumed to be condensing perpendicularly onto the condensed phase. Such an extension was required in connection with the general theory[33] to describe the vapor flow around an arbitrarily shaped condensed phase in the continuum limit when a small amount of the noncondensable gas is contained in the system.

The approach to the problem in the present paper is essentially the same as that in Ref. 24. After formulating the problem in Sec. II, we introduced the assumption that the molecules of the vapor and those of the noncondensable gas are mechanically identical in Sec. III. This assumption enables us to decompose the original problem into two problems, one for the total mixture, which is equivalent to the half-space problem of strong condensation for a pure vapor, and the other for the noncondensable gas. Taking advantage of this property, we discussed the general features of the

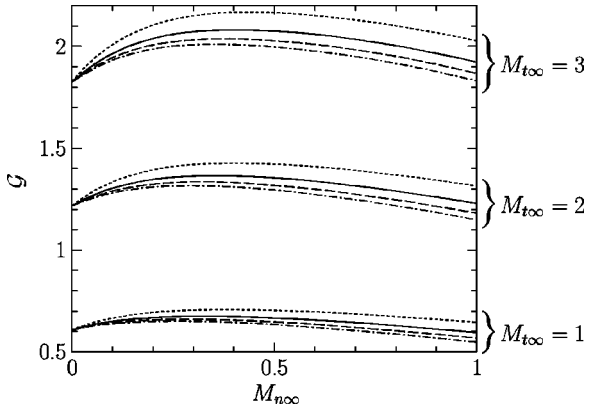

FIG. 9. $\mathcal{G}$ versus $M_{n\infty}$ for typical values of $M_{t\infty}$ and T_∞/T_w. See Table III. The dotted line indicates the result for $T_\infty/T_w=0.5$, the solid line for $T_\infty/T_w=1$, the dashed line for $T_\infty/T_w=1.5$, and the dotted–dashed line for $T_\infty/T_w=2$.

solution, in particular, the relation among the parameters that admits a steady solution (Sec. III). Then, we carried out actual numerical computations using the GSB model to obtain the numerical solution of the problem, in particular, the numerical data for the relation to be satisfied by the parameters (Sec. IV). In the present paper, we have restricted ourselves to the case of subsonic condensation, leaving the case of supersonic condensation in the subsequent paper. The numerical data of the relation provide the essential part of the numerical boundary condition for the Euler set of equations on the condensing boundary in the continuum limit.[33] Finally, we considered the half-space problem of strong evaporation in Sec. V and showed that the noncondensable gas cannot be present when evaporation is taking place in the case of Maxwellian molecules.

With the present numerical results incorporated as the boundary condition, the Euler system derived in Ref. 33 is now applicable to practical problems. Actually, such an example is already contained in Ref. 33. That is, the Euler system is applied to the analysis of the vapor flow evaporating from a plane condensed phase and condensing onto a wavy condensed phase of sinusoidal shape in the continuum limit, in the presence of a noncondensable gas of an infinitesimal average concentration. The result shows that such a trace of the noncondensable gas has a significant effect on the vapor flow. Further applications of the Euler system will be treated in a forthcoming paper.

APPENDIX A: COLLISION TERMS

The dimensionless collision term $\hat{J}^{\beta\alpha}$ is given as follows:

TABLE III. $\mathcal{G}(M_{n\infty}, M_{t\infty}, T_\infty/T_w)$ as a function of $M_{n\infty}$, $M_{t\infty}$, and T_∞/T_w.

	$T_\infty/T_w=0.5$				$T_\infty/T_w=1$			
$M_{n\infty}\backslash M_{t\infty}$	0	1	2	3	0	1	2	3
0.01	0	0.616 27	1.2326	1.8493	0	0.614 04	1.2282	1.8426
0.1	0	0.665 49	1.3341	2.0085	0	0.649 55	1.3033	1.9644
0.2	0	0.693 38	1.3932	2.1043	0	0.668 90	1.3464	2.0382
0.3	0	0.705 28	1.4199	2.1504	0	0.675 44	1.3635	2.0722
0.4	0	0.707 54	1.4270	2.1668	0	0.673 87	1.3643	2.0818
0.5	0	0.703 78	1.4220	2.1649	0	0.666 98	1.3545	2.0757
0.6	0	0.696 12	1.4092	2.1513	0	0.656 52	1.3376	2.0592
0.7	0	0.685 80	1.3910	2.1294	0	0.643 56	1.3157	2.0346
0.8	0	0.673 57	1.3688	2.1009	0	0.628 75	1.2897	2.0033
0.9	0	0.659 87	1.3433	2.0668	0	0.612 51	1.2603	1.9657
0.95	0	0.652 57	1.3295	2.0479	0	0.603 93	1.2445	1.9446
0.99	0	0.646 54	1.3180	2.0319	0	0.596 88	1.2313	1.9267
1	0	0.645 00	1.3151	2.0278	0	0.595 10	1.2279	1.9221
	$T_\infty/T_w=1.5$				$T_\infty/T_w=2$			
$M_{n\infty}\backslash M_{t\infty}$	0	1	2	3	0	1	2	3
0.01	0	0.613 05	1.2262	1.8397	0	0.612 45	1.2250	1.8379
0.1	0	0.642 05	1.2890	1.9443	0	0.637 46	1.2803	1.9323
0.2	0	0.656 81	1.3236	2.0064	0	0.649 27	1.3095	1.9869
0.3	0	0.660 08	1.3348	2.0326	0	0.650 29	1.3166	2.0076
0.4	0	0.655 97	1.3312	2.0372	0	0.644 35	1.3099	2.0084
0.5	0	0.646 99	1.3181	2.0280	0	0.633 82	1.2943	1.9967
0.6	0	0.634 70	1.2986	2.0095	0	0.620 19	1.2728	1.9767
0.7	0	0.620 10	1.2744	1.9836	0	0.604 39	1.2469	1.9498
0.8	0	0.603 76	1.2464	1.9510	0	0.586 97	1.2175	1.9164
0.9	0	0.586 07	1.2149	1.9118	0	0.568 27	1.1846	1.8763
0.95	0	0.576 79	1.1980	1.8898	0	0.558 52	1.1670	1.8538
0.99	0	0.569 20	1.1839	1.8711	0	0.550 56	1.1524	1.8346
1	0	0.567 28	1.1803	1.8663	0	0.548 55	1.1487	1.8297

$$\hat{J}^{\beta\alpha}(f,g)=\int [f(\zeta'_{*i})g(\zeta'_i)-f(\zeta_{*i})g(\zeta_i)] \times \hat{B}^{\beta\alpha}(|e_j\hat{V}_j|,|\hat{V}_i|)d\Omega(e_i)d^3\zeta_*, \tag{A1}$$

where

$$\zeta'_i=\zeta_i+\frac{\hat{\mu}^{\beta\alpha}}{\hat{m}^{\alpha}}(e_j\hat{V}_j)e_i, \quad \zeta'_{*i}=\zeta_{*i}-\frac{\hat{\mu}^{\beta\alpha}}{\hat{m}^{\beta}}(e_j\hat{V}_j)e_i, \tag{A2a}$$

$$\hat{\mu}^{\beta\alpha}=\frac{2\hat{m}^{\alpha}\hat{m}^{\beta}}{\hat{m}^{\alpha}+\hat{m}^{\beta}}, \quad \hat{m}^{\alpha}=m^{\alpha}/m^A, \tag{A2b}$$

$$\hat{V}_i=\zeta_{*i}-\zeta_i, \quad d^3\zeta_*=d\zeta_{*1}\,d\zeta_{*2}\,d\zeta_{*3}. \tag{A2c}$$

Here, e_i is a unit vector, ζ_{*i} is the variable of integration corresponding to ζ_i, $d\Omega(e_i)$ is the solid angle element in the direction of e_i, and $\hat{B}^{\beta\alpha}(|e_j\hat{V}_j|,|\hat{V}_i|)$ are nonnegative functions of $|e_j\hat{V}_j|$ and $|\hat{V}_i|$ depending on the molecular model. The domain of integration in Eq. (A1) is the whole space of ζ_{*i} and all directions of e_i.

We give further remarks on the function $\hat{B}^{\beta\alpha}$. The dimensional counterpart $B^{\beta\alpha}(|e_jV_j|,|V_i|)$ of $\hat{B}^{\beta\alpha}$, where

$$V_i=\xi_{*i}-\xi_i, \quad \xi_{*i}=(2kT_\infty/m^A)^{1/2}\zeta_{*i}, \tag{A3}$$

is such that the collision frequency $\nu^{\beta\alpha}$ of an α molecule for the collision with β molecules with the velocity distribution function F^{β} is expressed as

$$\nu^{\beta\alpha}=\int B^{\beta\alpha}(|e_jV_j|,|V_i|)F^{\beta}(\xi_{*i})d\Omega(e_i)d^3\xi_*, \tag{A4}$$

where $d^3\xi_*=d\xi_{*1}\,d\xi_{*2}\,d\xi_{*3}$, the domain of integration is the whole space of ξ_{*i} and all directions of e_i, and the arguments of F^{β} other than the molecular velocity are omitted. Let ν_∞ be the mean collision frequency (i.e., the inverse of the mean free time) of the vapor molecules in the equilibrium state at rest with number density n_∞ and temperature T_∞, which is related to the mean free path l_∞ by

$$\nu_\infty=(2/\sqrt{\pi})(2kT_\infty/m^A)^{1/2}/l_\infty. \tag{A5}$$

Then, ν_∞ is given by

$$\nu_\infty=\frac{1}{n_\infty}\int B^{AA}F_e^A(\xi_i)F_e^A(\xi_{*i})d\Omega(e_i)d^3\xi\,d^3\xi_*, \tag{A6a}$$

$$F_e^A(\xi_i)=\frac{n_\infty}{(2\pi kT_\infty/m^A)^{3/2}}\exp\left(-\frac{\xi_i^2}{2kT_\infty/m^A}\right), \tag{A6b}$$

where $d^3\xi=d\xi_1\,d\xi_2\,d\xi_3$, and the domain of integration is the whole space of ξ_i, that of ξ_{*i}, and all directions of e_i. The $\hat{B}^{\beta\alpha}$ in Eq. (A1) has been normalized as

$$\hat{B}^{\beta\alpha}(|e_j\hat{V}_j|,|\hat{V}_i|)=(n_\infty/\nu_\infty)B^{\beta\alpha}(|e_jV_j|,|V_i|). \tag{A7}$$

For Maxwellian molecules (see the second paragraph in Sec. V), $B^{\beta\alpha}$ is a function of $|e_jV_j|/|V_j|$ only; for hard-sphere molecules, $B^{\beta\alpha}$ is given explicitly by

$$B^{\beta\alpha}=(1/8)(d^{\beta}+d^{\alpha})^2|e_jV_j|, \tag{A8}$$

where d^{α} is the diameter of a molecule of α component. In the latter case, ν_∞, l_∞, and $\hat{B}^{\beta\alpha}$ are, respectively, obtained as

$$\nu_\infty=2\sqrt{2\pi}(2kT_\infty/m^A)^{1/2}(d^A)^2n_\infty, \tag{A9a}$$

$$l_\infty=[\sqrt{2}\pi(d^A)^2n_\infty]^{-1}, \tag{A9b}$$

$$\hat{B}^{\beta\alpha}=\frac{1}{4\sqrt{2\pi}}\left(\frac{d^{\beta}+d^{\alpha}}{2d^A}\right)^2|e_j\hat{V}_j|. \tag{A9c}$$

When the molecule of A component is mechanically identical with that of B component, we have $\hat{m}^{\alpha}=1$ and $\hat{B}^{\beta\alpha}=\hat{B}$, where $\hat{B}$ is independent of α and β. Then, $\hat{J}^{\beta\alpha}$ reduces to the following $\hat{J}$:

$$\hat{J}(f,g)=\int [f(\zeta'_{*i})g(\zeta'_i)-f(\zeta_{*i})g(\zeta_i)] \times \hat{B}(|e_j\hat{V}_j|,|\hat{V}_i|)d\Omega(e_i)d^3\zeta_*, \tag{A10}$$

with

$$\zeta'_i=\zeta_i+(e_j\hat{V}_j)e_i, \quad \zeta'_{*i}=\zeta_{*i}-(e_j\hat{V}_j)e_i. \tag{A11}$$

Note that $\hat{J}(f,f)$ is the (dimensionless) collision term of the Boltzmann equation for a single-component gas.

APPENDIX B: MODEL FOR COLLISION TERMS

In this appendix, we summarize the model collision term proposed by Garzó *et al.*[34] To be consistent with Eq. (2), we show it in the dimensionless form. The dimensionless collision term $\hat{J}^{\beta\alpha}(\hat{F}^{\beta},\hat{F}^{\alpha})$ in Eq. (2) is replaced by the following term:

$$\hat{J}^{\beta\alpha}(\hat{F}^{\beta},\ \hat{F}^{\alpha})=\hat{K}^{\beta\alpha}\hat{n}^{\beta}(\hat{F}^{\beta\alpha}-\hat{F}^{\alpha}), \tag{B1}$$

where

$$\hat{F}^{\beta\alpha}=\pi^{-3/2}\hat{n}^{\alpha}\left(\frac{\hat{m}^{\alpha}}{\hat{T}}\right)^{3/2}\exp\left(-\frac{\hat{m}^{\alpha}(\zeta_i-\hat{v}_i)^2}{\hat{T}}\right) \times\left\{1+2\frac{\hat{m}^{\alpha}}{\hat{T}}(\hat{v}_i^{\beta\alpha}-\hat{v}_i)(\zeta_i-\hat{v}_i)+\left[\frac{\hat{T}^{\beta\alpha}-\hat{T}}{\hat{T}}+\frac{2}{3}\frac{\hat{m}^{\alpha}}{\hat{T}} \times(\hat{v}_i^{\beta\alpha}-\hat{v}_i)^2\right]\left[\frac{\hat{m}^{\alpha}(\zeta_i-\hat{v}_i)^2}{\hat{T}}-\frac{3}{2}\right]\right\}, \tag{B2a}$$

$$\hat{v}_i^{\beta\alpha}=\frac{\hat{m}^{\alpha}\hat{v}_i^{\alpha}+\hat{m}^{\beta}\hat{v}_i^{\beta}}{\hat{m}^{\alpha}+\hat{m}^{\beta}}, \tag{B2b}$$

$$\hat{T}^{\beta\alpha}=\frac{\hat{m}^{\alpha}\hat{m}^{\beta}}{(\hat{m}^{\alpha}+\hat{m}^{\beta})^2}\left[\left(\frac{\hat{m}^{\alpha}}{\hat{m}^{\beta}}+\frac{\hat{m}^{\beta}}{\hat{m}^{\alpha}}\right)\hat{T}^{\alpha}+2\hat{T}^{\beta} +\frac{2}{3}\hat{m}^{\beta}(\hat{v}_i^{\alpha}-\hat{v}_i^{\beta})^2\right], \tag{B2c}$$

$$\hat{K}^{\beta\alpha}=K^{\beta\alpha}/K^{AA}, \tag{B2d}$$

and $K^{\beta\alpha}$ are constants. The collision frequency $\nu^{\beta\alpha}$ of the α molecules for their collisions with the β molecules is given by $\nu^{\beta\alpha}=K^{\beta\alpha}n^{\beta}$, and therefore, the mean free path l_∞ is

given by $l_\infty=(2/\sqrt{\pi})(2kT_\infty/m^A)^{1/2}/K^{AA}n_\infty$. The $\hat{n}^\alpha$, $\hat{T}^\alpha$, $\hat{v}_i^\alpha$, $\hat{T}$, and $\hat{v}_i$ in Eqs. (B1)–(B2c) are defined by Eqs. (10a)–(10f).

When the molecule of the vapor and that of the noncondensable gas are mechanically identical, we have

$$\hat{m}^\alpha=1, \quad \hat{K}^{\beta\alpha}=1. \tag{B3}$$

In this case, therefore, if we use Eq. (B1) in Eq. (2), then Eq. (14a) becomes the BGK model, that is, $\hat{J}(\hat{F},\hat{F})$ in Eq. (14a) reduces to

$$\hat{J}(\hat{F},\hat{F})=\hat{n}(\hat{F}_e-\hat{F}), \tag{B4}$$

where

$$\hat{F}_e=\pi^{-3/2}\frac{\hat{n}}{\hat{T}^{3/2}}\exp\left(-\frac{(\zeta_i-\hat{v}_i)^2}{\hat{T}}\right), \tag{B5a}$$

$$\hat{n}=\int \hat{F}\,d^3\zeta, \quad \hat{v}_i=\frac{1}{\hat{n}}\int \zeta_i\hat{F}\,d^3\zeta, \tag{B5b}$$

$$\hat{T}=\frac{2}{3\hat{n}}\int (\zeta_i-\hat{v}_i)^2\hat{F}\,d^3\zeta. \tag{B5c}$$

Correspondingly, $\hat{J}(\hat{F},\hat{F}^B)$ in Eq. (14b) reduces to

$$\hat{J}(\hat{F},\hat{F}^B)=\hat{n}(\hat{\Psi}_e-\hat{F}^B), \tag{B6}$$

where

$$\hat{\Psi}_e=\frac{\hat{n}^B}{\hat{n}}\hat{F}_e\left\{1-\frac{(\hat{v}_i-\hat{v}_i^B)(\zeta_i-\hat{v}_i)}{\hat{T}}-\frac{1}{2}\left[1-\frac{2}{3}\frac{(\hat{v}_i-\hat{v}_i^B)^2}{\hat{T}}-\frac{\hat{T}^B}{\hat{T}}\right]\left[\frac{(\zeta_i-\hat{v}_i)^2}{\hat{T}}-\frac{3}{2}\right]\right\}. \tag{B7}$$

If the definitions of $\hat{n}^B$, $\hat{v}_i^B$, and $\hat{T}^B$, i.e., Eqs. (10a)–(10c) with $\alpha=B$, are used, it turns out that $\hat{\Psi}_e$ is linear in $\hat{F}^B$.

APPENDIX C: DATA ON NUMERICAL COMPUTATION

The lattice systems used here are essentially the same as those used in Ref. 5 (see Appendix A of Ref. 5). But, in the present computation, the higher accuracy is attained basically by using wider computational regions, more lattice points, and smaller lattice intervals. The details of the lattice systems are omitted here.

The accuracy of the computation was checked in various ways. For many cases included in Tables V–VIII in Ref. 42 (the cases in Tables I–IV in Ref. 42 are all included in Tables V–VIII there), we carried out computation with finer lattice systems with double lattice points either in x_1 or in ζ_1 and confirmed that the values of F_s and Γ_* in Tables I and II (and Tables I–VIII in Ref. 42) did not change. More specifically, concerning the x_1 lattices, this check was performed for all $M_{n\infty}$ and for $M_{t\infty}=0$ and 3 in the cases included in Tables V–VIII in Ref. 42. The same check was also performed for many other cases in Tables V, VI, and VIII in Ref. 42. As for the ζ_1 lattices, the check was performed for about one third of the cases of Table VI in Ref. 42 and several cases for $M_{t\infty}=3$ of Tables V and VIII there. In general, accurate computation becomes more difficult as $M_{t\infty}$ increases. Although the lattice systems used in Ref. 5 are sufficient for obtaining $(\mathcal{H}_a,\ \mathcal{H}_b,\ \mathcal{H}_c)$ [cf. Eq. (26a)] and F_s accurately, we need higher accuracy to obtain accurate results for $(\mathcal{H}^B_{a*},\ \mathcal{H}^B_{b*},\ \mathcal{H}^B_{c*})$ [cf. Eq. (26b)] and Γ_*.

As in Ref. 5, the conservation laws were also used for checking the accuracy. Let us set

$$(I_1,\ I_2,\ I_3,\ I_4)=\int \zeta_1(1,\ \zeta_1,\ \zeta_2,\ \zeta_j^2)\hat{F}\,d^3\zeta, \tag{C1a}$$

$$I_1^B=\int \zeta_1\hat{F}^B\,d^3\zeta. \tag{C1b}$$

The $n_\infty(2kT_\infty/m^A)^{1/2}I_1$, $2p_\infty I_2$, $2p_\infty I_3$, and $p_\infty(2kT_\infty/m^A)^{1/2}I_4$ are, respectively, the number of molecules, the X_1 component of the momentum, its X_2 component, and the energy of the total mixture transported in the positive X_1 direction across a unit area of the plane $X_1=$const per unit time; $n_\infty(2kT_\infty/m^A)^{1/2}I_1^B$ is the molecular flux of the noncondensable gas corresponding to $n_\infty(2kT_\infty/m^A)^{1/2}I_1$. It was shown in Sec. II C that $I_1^B\equiv 0$. The integration of Eq. (14a) multiplied by $(1,\ \zeta_1,\ \zeta_2,\ \zeta_j^2)$ with respect to ζ_i over its whole space, under the condition (17a), yields

$$I_m=\text{const}=I_{m\infty} \quad (m=1,2,3,4), \tag{C2}$$

where $I_{m\infty}$ are the I_m at infinity and are given by

$$\begin{aligned} &I_{1\infty}=-(5/6)^{1/2}M_{n\infty}, \quad I_{2\infty}=[(5/3)M_{n\infty}^2+1]/2,\\ &I_{3\infty}=-(5/6)M_{n\infty}M_{t\infty},\\ &I_{4\infty}=-(5/6)^{3/2}M_{n\infty}(M_{n\infty}^2+M_{t\infty}^2+3). \end{aligned} \tag{C3}$$

Because of numerical error, I_m do not satisfy Eq. (C2) exactly and I_1^B does not vanish exactly. The deviations of the numerical values of $I_m-I_{m\infty}$ and I^B_{1*} from zero, where I^B_{1*} is the I_1^B with $\hat{F}^B=\hat{F}^B_*$ (see the first paragraph in Sec. III C), are estimated as follows:

$$|(I_m-I_{m\infty})/I_{m\infty}| \quad \text{and} \quad |I^B_{1*}/I_{1\infty}| < \begin{cases} 0.30\times10^{-4} & (M_{n\infty}=0.01),\\ 0.11\times10^{-4} & (0.03\leqslant M_{n\infty}\leqslant 0.07),\\ 0.22\times10^{-5} & (0.1\leqslant M_{n\infty}\leqslant 0.3),\\ 0.32\times10^{-6} & (0.4\leqslant M_{n\infty}), \end{cases} \tag{C4}$$

for all T_∞/T_w and $M_{t\infty}$ ($M_{t\infty}=0$ is excluded for $m=3$ because $I_3=I_{3\infty}=0$ in this case). The estimate naturally deteriorates for small $M_{n\infty}$ because $I_{1\infty}$, $I_{3\infty}$, and $I_{4\infty}$ in the denominator are proportional to $M_{n\infty}$.

[1] Y. Sone, "Kinetic theoretical studies of the half-space problem of evaporation and condensation," Transp. Theory Stat. Phys. **29**, 227 (2000).
[2] Y. Sone, *Kinetic Theory and Fluid Dynamics*, Modeling and Simulation in Science, Engineering and Technology (Birkhäuser, Boston, 2002).
[3] K. Aoki and Y. Sone, "Gas flows around the condensed phase with strong evaporation or condensation—Fluid dynamic equation and its boundary condition on the interface and their application—," in *Advances in Kinetic Theory and Continuum Mechanics*, edited by R. Gatignol and Soubbaramayer (Springer-Verlag, Berlin, 1991), p. 43.
[4] Y. Sone and H. Sugimoto, "Strong evaporation from a plane condensed

phase,'' in *Adiabatic Waves in Liquid-Vapor Systems*, edited by G. E. A. Meier and P. A. Thompson (Springer-Verlag, Berlin, 1990), p. 293.
[5]K. Aoki, K. Nishino, Y. Sone, and H. Sugimoto, ''Numerical analysis of steady flows of a gas condensing on or evaporating from its plane condensed phase on the basis of kinetic theory: Effect of gas motion along the condensed phase,'' Phys. Fluids A **3**, 2260 (1991).
[6]Y. Sone, K. Aoki, and I. Yamashita, ''A study of unsteady strong condensation on a plane condensed phase with special interest in formation of steady profile,'' in *Rarefied Gas Dynamics*, edited by V. Boffi and C. Cercignani (Teubner, Stuttgart, 1986), Vol. 2, p. 323.
[7]K. Aoki, Y. Sone, and T. Yamada, ''Numerical analysis of gas flows condensing on its plane condensed phase on the basis of kinetic theory,'' Phys. Fluids A **2**, 1867 (1990).
[8]P. L. Bhatnagar, E. P. Gross, and M. Krook, ''A model for collision processes in gases. I. Small amplitude processes in charged and neutral one-component systems,'' Phys. Rev. **94**, 511 (1954).
[9]P. Welander, ''On the temperature jump in a rarefied gas,'' Ark. Fys. **7**, 507 (1954).
[10]M. N. Kogan, ''On the equations of motion of a rarefied gas,'' Appl. Math. Mech. **22**, 597 (1958).
[11]Y. Sone, ''Kinetic theory of evaporation and condensation—Linear and nonlinear problems—,'' J. Phys. Soc. Jpn. **45**, 315 (1978).
[12]Y. Sone, F. Golse, T. Ohwada, and T. Doi, ''Analytical study of transonic flows of a gas condensing onto its plane condensed phase on the basis of kinetic theory,'' Eur. J. Mech. B/Fluids **17**, 277 (1998).
[13]M. N. Kogan and N. K. Makashev, ''Role of the Knudsen layer in the theory of heterogeneous reactions and in flows with surface reactions,'' Fluid Dyn. **6**, 913 (1971).
[14]M. Murakami and K. Oshima, ''Kinetic approach to the transient evaporation and condensation problem,'' in *Rarefied Gas Dynamics*, edited by M. Becker and M. Fiebig (DFVLR, Porz–Wahn, 1974), Vol. 2, F. 6-1.
[15]T. Ytrehus, ''Theory and experiments on gas kinetics in evaporation,'' in *Rarefied Gas Dynamics*, edited by J. L. Potter (AIAA, New York, 1977), p. 1197.
[16]M. N. Kogan and A. A. Abramov, ''Direct simulation solution of the strong evaporation and condensation problem,'' in *Rarefied Gas Dynamics*, edited by A. E. Beylich (VCH, Weinheim, 1991), p. 1251.
[17]A. P. Kryukov, ''Strong subsonic and supersonic condensation on a plane surface,'' in *Rarefied Gas Dynamics*, edited by A. E. Beylich (VCH, Weinheim, 1991), p. 1278.
[18]Y. Sone, S. Takata, and F. Golse, ''Notes on the boundary conditions for fluid-dynamic equations on the interface of a gas and its condensed phase,'' Phys. Fluids **13**, 324 (2001).
[19]A. V. Bobylev, R. Grzhibovskis, and A. Heintz, ''Entropy inequalities for evaporation/condensation problem in rarefied gas dynamics,'' J. Stat. Phys. **102**, 1151 (2001).
[20]M. D. Arthur and C. Cercignani, ''Non-existence of a steady rarefied supersonic flow in a half-space,'' Z. Angew. Math. Phys. **31**, 634 (1980).
[21]F. Coron, F. Golse, and C. Sulem, ''A classification of well-posed kinetic layer problems,'' Commun. Pure Appl. Math. **41**, 409 (1988).
[22]L. Arkeryd and A. Nouri, ''On the Milne problem and the hydrodynamic limit for a steady Boltzmann equation model,'' J. Stat. Phys. **99**, 993 (2000).
[23]S. Ukai, S.-H. Yu, and T. Yang, ''Nonlinear boundary layers of the Boltzmann equation,'' Commun. Math. Phys. (to be published).
[24]Y. Sone, K. Aoki, and T. Doi, ''Kinetic theory analysis of gas flows condensing on a plane condensed phase: Case of a mixture of a vapor and a noncondensable gas,'' Transp. Theory Stat. Phys. **21**, 297 (1992).
[25]K. Aoki and T. Doi, ''High-speed vapor flows condensing on a plane condensed phase in the presence of a noncondensable gas,'' in *Rarefied Gas Dynamics: Theory and Simulations*, edited by B. D. Shizgal and D. P. Weaver (AIAA, Washington, DC, 1994), p. 521.
[26]K. Aoki, S. Takata, and S. Kosuge, ''Vapor flows caused by evaporation and condensation on two parallel plane surfaces: Effect of the presence of a noncondensable gas,'' Phys. Fluids **10**, 1519 (1998).
[27]Y. Sone, ''Asymptotic theory of flow of rarefied gas over a smooth boundary I,'' in *Rarefied Gas Dynamics*, edited by L. Trilling and H. Y. Wachman (Academic, New York, 1969), Vol. 1, p. 243.
[28]Y. Sone, ''Asymptotic theory of flow of rarefied gas over a smooth boundary II,'' in *Rarefied Gas Dynamics*, edited by D. Dini (Editrice Tecnico Scientifica, Pisa, 1971), Vol. 2, p. 737.
[29]Y. Sone and Y. Onishi, ''Kinetic theory of evaporation and condensation—Hydrodynamic equation and slip boundary condition—,'' J. Phys. Soc. Jpn. **44**, 1981 (1978).
[30]Y. Onishi and Y. Sone, ''Kinetic theory of slightly strong evaporation and condensation—Hydrodynamic equation and slip boundary condition for finite Reynolds number—,'' J. Phys. Soc. Jpn. **47**, 1676 (1979).
[31]Y. Sone, ''Asymptotic theory of a steady flow of a rarefied gas past bodies for small Knudsen numbers,'' in *Advances in Kinetic Theory and Continuum Mechanics*, edited by R. Gatignol and Soubbaramayer (Springer-Verlag, Berlin, 1991), p. 19.
[32]Y. Sone, ''Theoretical and numerical analyses of the Boltzmann equation—Theory and analysis of rarefied gas flows—,'' *Lecture Notes* (Department of Aeronautics and Astronautics, Graduate School of Engineering, Kyoto University, 1998), Part I (http://www.users.kudpc.kyoto-u.ac.jp/~a50077/).
[33]K. Aoki, S. Takata, and S. Taguchi, ''Vapor flows with evaporation and condensation in the continuum limit: Effect of a trace of noncondensable gas,'' Eur. J. Mech. B/Fluids (to be published).
[34]V. Garzó, A. Santos, and J. J. Brey, ''A kinetic model for a multicomponent gas,'' Phys. Fluids A **1**, 380 (1989).
[35]G. A. Bird, *Molecular Gas Dynamics* (Oxford University Press, Oxford, 1976).
[36]G. A. Bird, *Molecular Gas Dynamics and the Direct Simulation of Gas Flows* (Oxford University Press, Oxford, 1994).
[37]Y. Sone and M. Sasaki (private communication).
[38]T. F. Morse, ''Kinetic model equations for a gas mixture,'' Phys. Fluids **7**, 2012 (1964).
[39]B. B. Hamel, ''Kinetic model for binary gas mixtures,'' Phys. Fluids **8**, 418 (1965).
[40]P. Andries, K. Aoki, and B. Perthame, ''A consistent BGK-type model for gas mixtures,'' J. Stat. Phys. **106**, 993 (2002).
[41]C. K. Chu, ''Kinetic-theoretic description of the formation of a shock wave,'' Phys. Fluids **8**, 12 (1965).
[42]See EPAPS Document No. E-PHFLE6-15-504303 for tables and figures. A direct link to this document may be found in the online article's HTML reference section. The document may also be reached via the EPAPS homepage (http://www.aip.org/pubservs/epaps.html) or from ftp.aip.org in the directory /epaps/. See the EPAPS homepage for more information.
[43]T. Doi, K. Aoki, and Y. Sone, ''Numerical analysis of unsteady evaporating flows from a plane condensed phase into a noncondensable gas on the basis of kinetic theory,'' J. Vac. Soc. Jpn. **37**, 143 (1994) (in Japanese).
[44]T. Doi, ''Numerical analysis of unsteady evaporating flows from a plane condensed phase into a noncondensable gas on the basis of kinetic theory II,'' J. Vac. Soc. Jpn. **38**, 203 (1995) (in Japanese).
[45]E. Goldman and L. Sirovich, ''Equations for gas mixtures,'' Phys. Fluids **10**, 1928 (1967).